

## Canopy-scale kinetic fractionation of atmospheric carbon dioxide and water vapor isotopes

Xuhui Lee,<sup>1</sup> Tim J. Griffis,<sup>2</sup> John M. Baker,<sup>2</sup> Kaycie A. Billmark,<sup>2</sup> Kyounghee Kim,<sup>1</sup> and Lisa R. Welp<sup>1</sup>

Received 18 August 2008; revised 16 October 2008; accepted 21 October 2008; published 4 February 2009.

[1] The carbon and oxygen isotopes of CO<sub>2</sub> and the oxygen isotopes of H<sub>2</sub>O are powerful tracers for constraining the dynamics of carbon uptake and water flux on land. The role of land biota in the atmospheric budgets of these isotopes has been extensively explored through the lens of leaf-scale observations. At the ecosystem scale, kinetic fractionation is associated with molecular and turbulent diffusion. Intuitively, air turbulence, being nondiscriminative in diffusing materials, should act to erase the kinetic effect. Using the first canopy-scale isotopic flux measurements, we show just the opposite: that in the terrestrial environment, air turbulence enhances the effect, rather than suppressing it. The sensitivity of kinetic fractionation to turbulence is striking in situations where the canopy resistance is comparable to or lower than the aerodynamic resistance. Accounting for turbulent diffusion greatly improves land surface model predictions of the isoforcing of <sup>18</sup>O-CO<sub>2</sub> and transpiration enrichment of leaf water in <sup>18</sup>O-H<sub>2</sub>O in field conditions. Our results suggest that variations in surface roughness across the landscape can contribute to spatial variations in the composition of atmospheric <sup>18</sup>O-CO<sub>2</sub> and that temporal trends in wind circulation on land can play a role in the interannual variability of atmospheric <sup>18</sup>O-CO<sub>2</sub>. In comparison, air turbulence has a limited effect on the isoforcing of <sup>13</sup>C-CO<sub>2</sub>.

**Citation:** Lee, X., T. J. Griffis, J. M. Baker, K. A. Billmark, K. Kim, and L. R. Welp (2009), Canopy-scale kinetic fractionation of atmospheric carbon dioxide and water vapor isotopes, *Global Biogeochem. Cycles*, 23, GB1002, doi:10.1029/2008GB003331.

### 1. Introduction

[2] The carbon and oxygen isotopes of CO<sub>2</sub> and the oxygen isotopes of H<sub>2</sub>O provide constraints on the temporal dynamics and spatial distributions of carbon uptake and water flux on land. At the global scale, the discrimination against <sup>13</sup>C-CO<sub>2</sub> by photosynthesis exerts an imprint on atmospheric <sup>13</sup>C-CO<sub>2</sub> that is uniquely different from the fossil and oceanic signals, allowing atmospheric models to partition ocean and land carbon fluxes [Battle *et al.*, 2000; Ciais *et al.*, 1995a]. Plant photosynthesis also plays an important part in the global budgets of <sup>18</sup>O in atmospheric O<sub>2</sub> and CO<sub>2</sub>. This is because O<sub>2</sub> released by photosynthesis and CO<sub>2</sub> that diffuses out of leaf stomata carry the <sup>18</sup>O signal of transpiration-enriched leaf water [Hoffmann *et al.*, 2004; Farquhar *et al.*, 1993]. Within the land biota, C<sub>3</sub> plants discriminate against <sup>13</sup>C more strongly and have generally higher efficiency of CO<sub>2</sub> hydration in the leaves than the C<sub>4</sub> plant group [Gillon and Yakir, 2001; Farquhar *et al.*, 1989]. Therefore, the <sup>13</sup>C and <sup>18</sup>O compositions of

atmospheric CO<sub>2</sub> contain information useful for inferring regional distributions of these biomes and their changes over time. At the ecosystem scale, a precise understanding of various discrimination processes helps researchers to unravel mechanisms that control the component fluxes of the net ecosystem carbon and water exchanges [Williams *et al.*, 2004; Ogée *et al.*, 2003; Bowling *et al.*, 2001].

[3] Land surface models (LSMs) provide a crucial bridge for linking the isotopic compositions of CO<sub>2</sub> and water in the atmosphere to biological activities on land. Some LSMs are embedded in global circulation models to quantify the land carbon sink [Ciais *et al.*, 1995] and atmospheric budgets of <sup>18</sup>O-H<sub>2</sub>O and <sup>18</sup>O-CO<sub>2</sub> [Hoffmann *et al.*, 2004; Cuntz *et al.*, 2003]. Others are driven by observed or model-derived meteorology to determine biome-specific discrimination factors across the world [Suits *et al.*, 2005; Randerson *et al.*, 2002; Gillon and Yakir, 2001; Lloyd and Farquhar, 1994; Farquhar *et al.*, 1993]. When run at the ecosystem scale, they offer new insights into mechanisms governing the isotopic exchange processes. LSM isotopic parameterizations are usually “trained” on leaf-scale observations, with a few exceptions where they are compared with field experimental data at the ecosystem scale [Chen and Chen, 2007; Aranibar *et al.*, 2006; Baldocchi and Bowling, 2003; Ogée *et al.*, 2003; Riley *et al.*, 2002; Kaplan *et al.*, 2002]. Validation of these parameterizations against field data

<sup>1</sup>School of Forestry and Environmental Studies, Yale University, New Haven, Connecticut, USA.

<sup>2</sup>Department of Soil, Water, and Climate, University of Minnesota, St. Paul, Minnesota, USA.

remains an area in need of more research [McDowell *et al.*, 2008].

[4] In recent years, our research groups have been developing in situ methods for measuring the isotopic fluxes of <sup>13</sup>C-CO<sub>2</sub>, <sup>18</sup>O-CO<sub>2</sub> and <sup>18</sup>O-H<sub>2</sub>O [Griffis *et al.*, 2005, 2008; Lee *et al.*, 2005]. One of our goals is to investigate processes that are not readily observable at the leaf scale but may be important for LSM parameterization of the isotopic exchange at the canopy scale in field conditions. In this paper, we focus our attention on the canopy-scale kinetic fractionation of these three isotopologues. Specifically, we are interested in understanding the relative role of turbulent and molecular diffusion in the kinetic effects at the canopy scale. Underpinning our analysis is the big-leaf framework in which the whole canopy is treated as one single entity and gaseous diffusion follows the resistance analogue described with a number of bulk resistance terms. A complete isotopic LSM to include these canopy-scale effects is under development and will be published at a later date.

[5] The present study is motivated in part by the inconsistent treatment in the published literature of the kinetic effect on <sup>18</sup>O-H<sub>2</sub>O between the terrestrial and marine environments. In the classic paper by Craig and Gordon [1965], the transport of water vapor from a water surface consists of molecular diffusion in a thin laminar layer in contact with the surface and nondiscriminating turbulent diffusion in a turbulent layer aloft. The total kinetic effect on <sup>18</sup>O-H<sub>2</sub>O is found to be ~20% of its molecular value of 32 per mil (their equation (30)). Adopting Brutsaert's theory on local evaporation [Brutsaert, 1975], Merlivat and Jouzel [1979] showed that the kinetic factor  $\epsilon_k^w$  of evaporation depends on the roughness of the water surface, varying from 6–7 per mil in the smooth regime to 2.5–4 per mil in the rough regime. In a laboratory investigation of pan evaporation, Cappa *et al.* [2003] found that  $\epsilon_k^w$  is 35% of the molecular value or 11 per mil.

[6] In the investigation of the vapor isotopic exchange between vegetation and the atmosphere, the kinetic fractionation is considered to be a process dominated by molecular diffusion. At the leaf scale,  $\epsilon_k^w$  is a resistance-weighted mean of the molecular value associated with the stomatal pathway and that in the leaf boundary layer [Farquhar and Lloyd, 1993; Flanagan *et al.*, 1991; Dongmann *et al.*, 1974]. Because the stomatal resistance is usually much greater than the leaf boundary layer resistance, the overall  $\epsilon_k^w$  is close to the molecular value. The prediction of the leaf water enrichment with this kinetic factor is in good agreement with observations so long as air humidity and the vapor isotope content, two critical inputs to the Craig-Gordon model, are measured in the vicinity of the leaf boundary layer [e.g., Flanagan *et al.*, 1991; Roden and Ehleringer, 1999]. When the leaf-scale analysis is extended to global-scale modeling,  $\epsilon_k^w$  is allowed to vary slightly to account for the leaf boundary layer effect [Farquhar *et al.*, 1993; Ciais *et al.*, 1997; Cuntz *et al.*, 2003; Hoffmann *et al.*, 2004]. In these modeling studies,  $\epsilon_k^w$  varies from 26.0 to 26.3 per mil, which is much higher than the values of 2.5–11 per mil considered appropriate for evaporation over water surfaces. That gaseous diffusion in a vegetated landscape also goes through turbulent pathways,

such as the canopy airspace and the atmospheric surface layer, begs the question of whether the  $\epsilon_k^w$  values used in these modeling studies are too high. Similar concerns can be raised for <sup>13</sup>C-CO<sub>2</sub> and <sup>18</sup>O-CO<sub>2</sub> as turbulent diffusion is expected to play a role in the kinetic fractionation of these isotopes.

[7] Several investigators have noted the role of turbulent diffusion in the vegetation-air isotopic exchange processes. Dongmann *et al.* [1974] suggested that  $\epsilon_k^w$  in a fully turbulent aerodynamic layer should be constant at 16 per mil, which they considered to be the lower limit associated with plant transpiration. Riley *et al.* [2002] separated the transpiration pathway into a molecular part (from the stomatal cavity to the canopy airspace) and a turbulent part (from the canopy airspace to the surface layer). The kinetic effects in their study are confined to the first part and are determined with the resistance-weighting method. Ogee *et al.* [2003] used the resistance-weighting method for <sup>13</sup>C-CO<sub>2</sub> assuming that the aerodynamic pathway discriminates against <sup>13</sup>C-CO<sub>2</sub> in the same fashion as the leaf boundary layer. In this study, we wish to refine these ideas with our recently acquired data sets on the canopy-scale isotopic fluxes. A unique feature of the data is that simultaneous and continuous observations were made of <sup>13</sup>C-CO<sub>2</sub>, <sup>18</sup>O-CO<sub>2</sub> and <sup>18</sup>O-H<sub>2</sub>O, allowing us to examine the kinetic effects on the three isotopologues in a consistent manner.

[8] This paper is organized as follows. Using the isoforcing concept, we present in section 2 a derivation of the canopy-scale kinetic factors and a big-leaf parameterization of the land-air isotopic fluxes. The data sets used for this study are described in section 3; they consist of observations made in a soybean and a mixed forest ecosystem whose level of turbulence differs substantially because of a large difference in surface roughness. In section 4, we compare the observed ecosystem isoforcing with that predicted by the big-leaf parameterization with and without considering turbulent diffusion in the kinetic effects. This is followed by a discussion in section 5 on the implications of the canopy kinetic mechanism for local- and global-scale studies of isotopic budgets in the atmosphere. A list of symbol definitions can be found in the notation section and resistance formulae are given in Appendix A.

## 2. Theory

### 2.1. Isoforcing on the Atmosphere

[9] Let  $\delta$  be the isotopic composition of CO<sub>2</sub> and H<sub>2</sub>O in delta notation

$$\delta = \left( \frac{R}{R_s} - 1 \right) \times 1000 \quad \text{per mil},$$

where  $R = c_i/c$  is the molar ratio,  $c_i$  and  $c$  are the mixing ratio of the minor and major isotopologue, respectively, and  $R_s$  is the VSMOW standard for water and VPDB standard for CO<sub>2</sub>. In the atmospheric boundary layer,  $\delta$  is a conservative tracer governed by the following conservation equation

$$\frac{\partial \bar{\delta}}{\partial t} + \frac{\partial \bar{u} \bar{\delta}}{\partial x} + \frac{\partial \bar{v} \bar{\delta}}{\partial y} + \frac{\partial \bar{w} \bar{\delta}}{\partial z} + \frac{\partial \bar{u}' \delta'}{\partial x} + \frac{\partial \bar{v}' \delta'}{\partial y} + \frac{\partial \bar{w}' \delta'}{\partial z} = 0, \quad (1)$$

where overbar denotes Reynolds or time averaging, prime denotes departure from the time average, and  $\{u, v, w\}$  are the three velocity components in the  $\{x, y, z\}$  directions. In the case of the vapor  $\delta$ , we assume a boundary layer without cloud formation to change  $\delta$ . In the absence of advection, equation (1) is reduced to

$$\frac{\partial \bar{\delta}}{\partial t} + \frac{\partial \overline{w'\delta'}}{\partial z} = 0. \quad (2)$$

Therefore the local time rate of change in  $\delta$  is balanced exactly by the vertical divergence of  $\overline{w'\delta'}$ . The relationship between  $\delta$  and the covariance term  $\overline{w'\delta'}$  (in units of per mil m s<sup>-1</sup>) is equivalent to that between the mixing ratio  $c$  and  $\overline{w'c'}$ , the eddy covariance flux of  $c$ .

[10] Physically, the covariance term  $\overline{w'\delta'}$  can be interpreted in the same way as the eddy flux of any other scalar in the atmosphere. Let us consider, for example, air movement over vegetation in the daytime growing season condition. An upward moving air parcel with positive  $w'$ , being originated from the canopy airspace, is usually more enriched in <sup>18</sup>O-CO<sub>2</sub> than a downward moving parcel with negative  $w'$ . The positive correlation between  $w$  and  $\delta$  will cause the  $\delta$  of the air layer aloft to increase with time.

[11] We now show that  $\overline{w'\delta'}$  is an appropriate flux for the study of land-air isotopic exchange. According to the theoretical analysis of *Cuntz et al.* [2003], *Tans* [1980], and others, for the calculation of the  $\delta$  budget in the atmosphere the flux boundary condition at the land-air interface is given by an isoforcing term expressed as

$$\text{Isoforcing} = \frac{F}{C_a} (\delta_F - \delta_a), \quad (3)$$

where  $F$  is the flux of  $c$  in units of  $\mu\text{mol m}^{-2}\text{s}^{-1}$ ,  $C_a$  is the molar concentration of  $c$  in units of  $\mu\text{mol m}^{-3}$ , and  $\delta_a$  is the isotopic composition in ambient air. Mathematically,  $\overline{w'\delta'}$  is identical to the isoforcing on the atmosphere. This can be demonstrated by expressing the Reynolds fluctuation of  $R$  from its temporal average  $\bar{R}$  as

$$R' = \frac{c'_i}{\bar{c}} - \frac{\bar{c}_i}{\bar{c}^2} c' = \frac{1}{\bar{c}} (c'_i - \bar{R} c'),$$

where higher-order terms are ignored. The covariance between  $w$  and  $R$  can be written as

$$\overline{w'R'} = \frac{\overline{w'c'_i}}{\bar{c}} \left( \frac{\overline{w'c'_i}}{\overline{w'c'}} - \bar{R} \right). \quad (4)$$

The two terms in the parentheses on the right of equation (4) are related to their counterparts in the  $\delta$  notation as

$$\delta_F = \left( \frac{\overline{w'c'_i}}{\overline{w'c'}} / R_s - 1 \right) \times 1000 \quad (5)$$

$$\delta_a = (\bar{R}/R_s - 1) \times 1000. \quad (6)$$

We also note that

$$\delta' = \frac{R'}{R_s} \times 1000. \quad (7)$$

Making use of equations (5)–(7), we can convert equation (4) to the  $\delta$  notation as

$$\overline{w'\delta'} = \frac{F}{C_a} (\delta_F - \delta_a). \quad (8)$$

Therefore the covariance term  $\overline{w'\delta'}$  represents the ecosystem-scale isoforcing on the atmosphere. Direct measurement of  $\overline{w'\delta'}$  can now be made with eddy covariance using laser-based technology [*Griffis et al.*, 2008].

[12] Equation (8) is the point of departure for the big-leaf parameterization presented below. It is related to several important concepts in the published literature on the isotopic exchange over land. In the case of leaf-air CO<sub>2</sub> exchange, the difference  $\delta_F - \delta_a$  is nearly identical to the photosynthetic discrimination factor  $\Delta$  except that the sign is reversed. At the ecosystem scale, the concept of isoflux, defined as the product of  $F$  and  $\delta_F$ , brings an additional equation to constrain the problem of partitioning the net ecosystem flux to its component fluxes [*Riley et al.*, 2002; *Bowling et al.*, 2001]. It has the same dimensions as  $C_a \overline{w'\delta'}$  but differs from the latter by an additional term  $F\delta_a$ . If the goal is to determine the isotopic budget of canopy air, a one-way flux term should be added to the isoforcing associated with photosynthesis and respiration [*Lloyd et al.*, 1996]. On the global scale, a disequilibrium isoflux results from the imbalance between the photosynthetic and respiration isoforcing, causing the atmospheric  $\delta$  to adjust accordingly [*Battle et al.*, 2000].

[13] In section 4, both  $\overline{w'\delta'}$  and  $C_a(\overline{w'\delta'})$  will be used. The former is termed as *isoforcing* and is the correct flux boundary condition driving the temporal variability of  $\delta_a$  in air (equations (3) and (8)). The latter carries the eddy isoflux dimensions of  $\mu\text{mol m}^{-2}\text{s}^{-1}$  per mil as noted above and will be referred to as *eddy isoforcing*.

## 2.2. Canopy-Scale Kinetic Factors

[14] The kinetic effects arise from the fact that molecular diffusivity differs between the major ( $c$ ) and minor ( $c_i$ ) isotopologues. Let  $r$  and  $r_i$  be the diffusion resistance to  $c$  and  $c_i$ , respectively. Their relationship can be expressed as

$$(r_i/r) = (D/D_i) \quad (9)$$

where  $D_i$  and  $D$  are molecular diffusivity of the minor and major isotopologues in air, respectively. The kinetic factor associated with resistance  $r$  is given as

$$\epsilon_k = n(1 - D_i/D) \times 1000 \quad \text{per mil.} \quad (10)$$

The exponent  $n$  takes the value of zero in the limit of fully turbulent diffusion, 2/3 for diffusion through the leaf laminar boundary layer, and unity in the limit of fully molecular diffusion [*Craig and Gordon*, 1965; *Merlivat and Jouzel*, 1979; *Farquhar and Lloyd*, 1993]. In the big-leaf

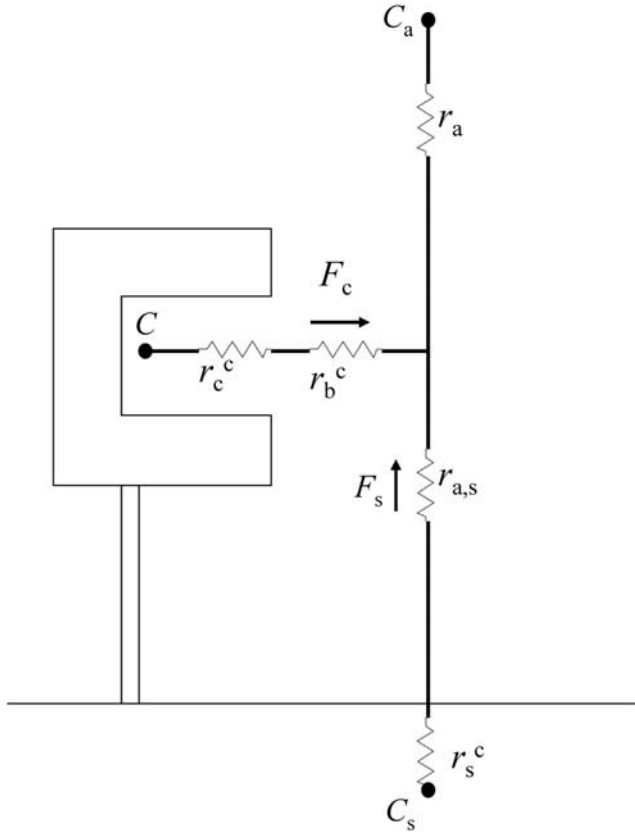


**Figure 1.** Big-leaf representation of the carbon dioxide exchange pathways in a canopy. Variable definitions are given in the notation section.

framework (Figure 1),  $n$  equals unity for diffusion associated with the canopy resistance  $r_c$ , zero with the aerodynamic resistance  $r_a$ , and  $2/3$  with the bulk leaf boundary layer resistance  $r_b$ .

[15] We now use  $^{18}\text{O}\text{-CO}_2$  to demonstrate the derivation of the kinetic fractionation factor at the canopy scale. Using the resistance analogy (Figure 1), we can rewrite equation (4) as

$$\overline{(w'R)}_c^{18} = \frac{F_c}{C_a} \left[ k \frac{R_c^{18} C - R_a^{18} C_a}{C - C_a} - R_a^{18} \right], \quad (11)$$

where subscript  $c$  denotes the canopy exchange,  $F_c$  is the canopy flux of  $\text{CO}_2$ ,  $R_c^{18}$  and  $R_a^{18}$  are the  $^{18}\text{O}/^{16}\text{O}\text{-CO}_2$  molar ratio in the intercellular space and in air at a reference height  $z_m$  above the canopy, respectively, and

$$k = \frac{r_a + r_b^c + r_c^c}{r_a + r_b^c + r_c^c}. \quad (12)$$

In delta notation, equation (11) becomes

$$\overline{(w'\delta')}^18_c = \frac{F_c}{C_a} \left[ \frac{C}{C - C_a} (\delta_c^{18} - \delta_a^{18}) - \epsilon_k^{18} \right], \quad (13)$$

where  $\epsilon_k^{18}$ , the canopy-scale kinetic fractionation factor for  $^{18}\text{O}\text{-CO}_2$ , is given by

$$\epsilon_k^{18} = 1000(1 - k) \text{ per mil.} \quad (14)$$

Combining equations (12) and (14) and making use of  $1000(r_{b,i}^c/r_b^c - 1) = 8.8 \times 2/3 = 5.8$  per mil and  $1000(r_{c,i}^c/r_c^c - 1) = 8.8$  per mil, equation (14) can be rearranged to give

$$\epsilon_k^{18} = \frac{5.8r_b^c + 8.8r_c^c}{r_a + r_b^c + r_c^c}. \quad (15)$$

[16] The same derivation can be extended to  $^{13}\text{C}\text{-CO}_2$  and  $^{18}\text{O}\text{-H}_2\text{O}$  to obtain their kinetic fractionation factors at the canopy scale,

$$\epsilon_k^{13} = \frac{2.9r_b^c + 4.4r_c^c}{r_a + r_b^c + r_c^c} \quad (16)$$

$$\epsilon_k^w = \frac{21r_b^w + 32r_c^w}{r_a + r_b^w + r_c^w}, \quad (17)$$

where the molecular kinetic factor is 4.4 per mil for  $^{13}\text{C}\text{-CO}_2$  and 32 per mil for  $^{18}\text{O}\text{-H}_2\text{O}$  [Cappa et al., 2003; Farquhar et al., 1989].

[17] Several salient points deserve the reader's attention here. First, the above derivation is not new; it is a simple extension of the leaf derivation to the canopy scale [Farquhar et al., 1993; Flanagan et al., 1991]. Second, only in the unrealistic limit of  $r_a = 0$  do equations (15)–(17) reduce to the familiar, leaf-scale forms, which for  $^{18}\text{O}\text{-CO}_2$  and  $^{18}\text{O}\text{-H}_2\text{O}$  are given as

$$\epsilon_k^{18} = \frac{5.8r_b^c + 8.8r_c^c}{r_b^c + r_c^c} \quad (18)$$

$$\epsilon_k^w = \frac{21r_b^w + 32r_c^w}{r_b^w + r_c^w}. \quad (19)$$

Third, some researchers determine the kinetic effects by applying weighting factors according to the conductance and concentration values at various points along the diffusion pathway [e.g., Cernusak et al., 2004; Flanagan et al., 1991]. We prefer the resistance weighting method because these resistance terms can be determined with the standard procedure found in the LSM literature (see Appendix A).

## 2.3. Isoforcing Parameterization

### 2.3.1. $^{18}\text{O}\text{-CO}_2$ Isoforcing

[18] To parameterize the  $^{18}\text{O}\text{-CO}_2$  isoforcing, we use the additive or linear superposition principle to divide the whole-ecosystem isoforcing  $(w'\delta')^{18}$  into canopy  $[(w'\delta')_c^{18}]$  and soil  $[(w'\delta')_s^{18}]$  components, as

$$\overline{(w'\delta')}^18 = \overline{(w'\delta')}^18_c + \overline{(w'\delta')}^18_s. \quad (20)$$

The two isoforcing components are parameterized separately. The canopy isoforcing can be calculated according to equation (13) if CO<sub>2</sub> in the intercellular space is in full equilibrium with the laminar leaf water, that is,

$$\delta_c^{18} = \delta_e^{18}.$$

More generally, the extent of CO<sub>2</sub> hydration in leaves ( $\theta_{eq}$ ) is less than unity. Applying the method of *Gillon and Yakir* [2001] to the canopy, we obtain the canopy isoforcing parameterization

$$\left(\overline{w'\delta'}\right)_c^{18} = \frac{F_c}{C_a} \left[ \frac{C}{C - C_a} (\delta_e^{18} - \delta_a^{18}) \theta_{eq} + (1 - \theta_{eq}) \epsilon_k^{18} \frac{C}{C_a} - \epsilon_k^{18} \right]. \quad (21)$$

In our calculation, estimates of  $\theta_{eq}$  were taken from *Gillon and Yakir* [2000b, 2001] ( $\theta_{eq} = 0.75$  for the soybean ecosystem and 0.96 for the forest). Equation (21) omits the impact of gross fluxes at the time when the net flux  $F_c$  is zero.

[19] The equilibrium value  $\delta_e^{18}$  is given by

$$\delta_e^{18} = \delta_L^w + 17604 / (T_c + 273.16) - 17.93,$$

where  $T_c$  is canopy temperature and  $\delta_L^w$  is the <sup>18</sup>O isotopic composition of water at the evaporating site within the leaf. In this equation,  $\delta_L^w$  has been converted from the VSMOW to the VPDB scale. The Craig-Gordon model is used to predict  $\delta_L^w$  on the assumption that transpiration is at steady state. The inputs to the model include the canopy-scale kinetic factor (equation (17)), the vapor isotope ratio and humidity at the reference height  $z_m$ , canopy temperature and the xylem water <sup>18</sup>O-H<sub>2</sub>O composition. In a thorough evaluation of the steady state assumption, we found that the Craig-Gordon model calculation is in very good agreement in midday with estimates based on the measured <sup>18</sup>O-H<sub>2</sub>O composition of canopy transpiration [*Welp et al.*, 2008]. At night and during sunrise and sunset transitions, the steady state assumption may be in error but its impact on the isoforcing calculation is limited because of the small canopy CO<sub>2</sub> flux at these times.

[20] In equation (21), the first term in the square brackets is dominant. It describes the mechanism of biological discrimination against <sup>18</sup>O-CO<sub>2</sub>. In the daytime photosynthetic phase, plants draw CO<sub>2</sub> from the atmosphere to the canopy ( $F_c < 0$ ), maintaining a negative CO<sub>2</sub> gradient along the gaseous diffusion pathway ( $C - C_a < 0$ ). Simultaneously, the transpiration-enriched <sup>18</sup>O signal of the leaf water ( $\delta_L^w$ ) is passed to CO<sub>2</sub> in the intercellular space through the hydration reaction, creating a positive isotopic gradient ( $\delta_e^{18} - \delta_a^{18} > 0$ ), typically on the order of 2 to 10 per mil. Taken together, these factors result in a positive isoflux whose effect is to enrich the air in <sup>18</sup>O-CO<sub>2</sub>. At night, canopy and soil respiration usually depletes the <sup>18</sup>O-CO<sub>2</sub> signature in air ( $(\overline{w'\delta'})^{18} < 0$ ) [see *Cernusak et al.*, 2004; *Seibt et al.*, 2007].

[21] Similarly, the isoforcing of soil respiration can be parameterized as

$$\left(\overline{w'\delta'}\right)_s^{18} = \frac{F_s}{C_a} \left[ \frac{C_s}{C_s - C_a} (\delta_s^{18} - \delta_a^{18}) - \epsilon_{k,s}^{18} \right], \quad (22)$$

where  $F_s$  is the soil CO<sub>2</sub> flux,  $C_s$  is the CO<sub>2</sub> concentration in soil air and  $\delta_s^{18}$  is its isotopic composition assumed to be in full equilibrium with soil water whose isotopic composition is interpolated between weekly measurements at a depth of 10 cm. The kinetic fractionation factor for soil respiration,  $\epsilon_{k,s}^{18}$ , is given by

$$\epsilon_{k,s}^{18} = \frac{8.8r_s^c}{r_a + r_{a,s} + r_s^c},$$

where  $r_{a,s}$  is the aerodynamic resistance in the canopy airspace, and  $r_s^c$  is the resistance to CO<sub>2</sub> diffusion in the soil pore space. The resistance analogy accounts for the effect of air invasion into the soil [*Tans*, 1998].

[22] The soil CO<sub>2</sub> flux,  $F_s$ , is calculated according to a Q<sub>10</sub>-type regression model established on the basis of soil chamber observations at the experimental sites. The canopy CO<sub>2</sub> flux is given by  $F_c = F - F_s$ , where the whole-ecosystem flux,  $F$ , was measured with the EC method. The CO<sub>2</sub> molar concentrations in the intercellular space and in soil air are given by

$$C = C_a + F_c(r_a + r_b^c + r_c^c)$$

$$C_s = C_a + F_s(r_a + r_{a,s} + r_s^c).$$

### 2.3.2. <sup>13</sup>C-CO<sub>2</sub> Isoforcing

[23] Similar to <sup>18</sup>O-CO<sub>2</sub>, the whole-ecosystem <sup>13</sup>C-CO<sub>2</sub> isoforcing consists of two components

$$\left(\overline{w'\delta'}\right)^{13} = \left(\overline{w'\delta'}\right)_c^{13} + \left(\overline{w'\delta'}\right)_s^{13}. \quad (23)$$

The canopy isoforcing is given by

$$\left(\overline{w'\delta'}\right)_c^{13} = -\frac{F_c}{C_a} \left[ \epsilon_k^{13} + (b - \epsilon_k^{13}) \frac{C}{C_a} \right], \quad (24)$$

where  $b$  is the <sup>13</sup>C discrimination factor in the carboxylation reaction (=27 per mil) [*Farquhar et al.*, 1989]. The soil isoforcing is given by

$$\left(\overline{w'\delta'}\right)_s^{13} = \frac{F_s}{C_a} (\delta_R^{13} - \delta_a^{13}), \quad (25)$$

where  $\delta_R^{13}$  is the <sup>13</sup>C-CO<sub>2</sub> isotopic composition of soil respiration (=−22 per mil for the soybean ecosystem [*Griffis et al.*, 2007]). The <sup>13</sup>C-CO<sub>2</sub> isoforcing calculation was made for the soybean ecosystem only.

## 3. Experimental Data

### 3.1. Soybean Experiment

[24] Details of the soybean experiment have been reported elsewhere [*Griffis et al.*, 2008; *Welp et al.*, 2008]. The experiment was conducted at the University of Minnesota Rosemount Research and Outreach Center located near St. Paul, Minnesota, United States, in 2006. The site was managed in a corn-soybean rotation. The experiment was conducted during the soybean (*Glycine max*) phase of the

rotation with planting taking place on 24 May. The peak leaf area index ( $L$ ) of 8.1 occurred on day of year (DOY) 215. The maximum canopy height ( $h$ ) was 1.0 m.

[25] A unique feature of the experiment was that three tunable diode laser analyzers were deployed to measure simultaneously the isotopic compositions and fluxes of <sup>18</sup>O-H<sub>2</sub>O, <sup>13</sup>C-CO<sub>2</sub> and <sup>18</sup>O-CO<sub>2</sub>. Two analyzers, operated continuously from May to September, measured the vertical gradient of the composition of these isotopes over the canopy. The third analyzer was used in conjunction with a sonic anemometer to measure the whole-ecosystem isotopic fluxes of <sup>13</sup>C-CO<sub>2</sub> and <sup>18</sup>O-CO<sub>2</sub>, using the closed-path eddy covariance (EC) method, in the later part of the growing season. Both the ecosystem isoforcing  $w'\delta'$  described in section 2.1 and the conventional isoflux defined by *Bowling et al.* [2001] were computed from the isotopic EC measurement. The flux ratios measured with the EC method were in excellent agreement with those determined with the gradient diffusion method. Because of tube attenuation, the CO<sub>2</sub> flux measured with the laser EC system was underestimated by 10% in comparison to an open-path EC. In this study, a 10% correction was applied to the isoforcing of <sup>13</sup>C-CO<sub>2</sub> and <sup>18</sup>O-CO<sub>2</sub> to account for the tube effect according to equation (8).

[26] In support of the interpretation of the isotopic flux data, we made measurements of leaf water  $\delta$  with leaves from the upper and the lower layers of the canopy. The sampling was made once a day at midday, except in rainy weather when no measurement was made and in a 3-day intensive campaign when the measurement was made every 4 h. We also made weekly  $\delta$  measurements of xylem water and 10-cm soil water, event-based precipitation and periodic measurements of groundwater. Other supporting measurements include the whole-ecosystem fluxes of CO<sub>2</sub>, latent heat, sensible heat and momentum, wind speed, air temperature and humidity, all at a reference height ( $z_m$ ) of 3.0 m above the ground. Canopy temperature was determined from the measurement of the outgoing longwave radiation.

### 3.2. Mixed Forest Experiment

[27] The experiment was conducted in a mixed forest in Connecticut, United States, from May to early November 2005. Details of the experiment can be found in the work of *Lee et al.* [2007]. The dominant overstory tree species were red maple (*Acer rubrum*), eastern white pine (*Pinus strobus*), beech (*Fagus grandifolia*), and hemlock (*Tsuga canadensis*). Mean tree height was 16–20 m. The average annual temperature was 7.0°C. The average total annual precipitation was 133 cm. The growing season LAI was about 4. Even though this experiment was not as comprehensive as the soybean experiment, it provided valuable insights into the kinetic effects because of its very different surface roughness. Additionally, it included isotopic measurements of the source (soil and xylem) water and water vapor, two critical variables for the <sup>18</sup>O-CO<sub>2</sub> isoforcing parameterization.

[28] The <sup>18</sup>O composition of atmospheric vapor was measured at two heights (21.7 and 30.7 m above the ground) over the treetops using one tunable-diode analyzer. The measurement was continuous except for a 1-week gap

due to pump failure. The ecosystem CO<sub>2</sub> and water vapor fluxes and other micrometeorological variables were measured at  $z_m = 30.4$  m above the ground. No measurement of <sup>18</sup>O-CO<sub>2</sub> and <sup>13</sup>C-CO<sub>2</sub> was available at the site. To compute the <sup>18</sup>O-CO<sub>2</sub> isoforcing (equations (21) and (22)), we assume that the <sup>18</sup>O-CO<sub>2</sub> composition in air followed the seasonal trend recorded at Park Falls by the NOAA flask network (<http://www.esrl.noaa.gov/gmd/ccgg/iadv/>). A diurnal variation was superimposed on the trend according to the seasonal composite measured at the soybean site. All other variables in equations (21) and (22) were obtained from the measurement at the site.

[29] Conventional isotopic measurements were made to characterize ecosystem water pools. They included rain (event basis), xylem water (biweekly) and soil water (every 3–7 days). No measurement of the leaf water  $\delta$  was available. But we note that the Craig-Gordon prediction was in the range of 7–9 per mil reported by the MIBA network for temperate forests in the northeastern United States (<http://public.ornl.gov/ameriflux/resource/meetingworkshops.shtml>).

[30] The Craig-Gordon model requires that the relative humidity measured at the reference height be expressed in reference to the canopy temperature,  $T_c$ . In this experiment, no measurement of  $T_c$  was available; instead,  $T_c$  was inferred from the aerodynamic principle, as

$$T_c = T_a + (\overline{w'T'})r_t,$$

where  $r_t$  was calculated according to the procedure described in Appendix A.

## 4. Results

[31] Figure 2 is a time series plot of  $\delta_v$  and  $\delta_a^{18}$  in the surface layer and  $\delta_L^w$  predicted by the Craig-Gordon model for a 9-day period in the peak soybean growing season. The diurnal cycle of  $\delta_a^{18}$  was more or less in phase with  $\delta_L^w$ , indicating the dominant role of canopy processes in the budget of <sup>18</sup>O-CO<sub>2</sub> in surface air. The low  $\delta_a^{18}$  (−5.9 per mil) on DOY 215 coincided with the low  $\delta_L^w$  caused by the unseasonably low  $\delta_v$  (−20.7 per mil).

[32] Figure 3a presents a comparison of the measured eddy <sup>18</sup>O-CO<sub>2</sub> isoforcing,  $C_a (w'\delta')^{18}$ , with the big-leaf calculation according to equations (20)–(22) for the same period shown in Figure 2. Quantities on the right side of equations (21) and (22) were either measured in the field or determined with schemes commonly used in land surface modeling (see Appendix A), with no tuneable parameters allowed. Most notably, the real-time measurement of  $\delta_v$  was used in the Craig-Gordon model to compute  $\delta_L^w$ ; the assumption of a constant  $\delta_v$  or a value in equilibrium with the xylem water would have missed the highly dynamic behaviors of  $\delta_L^w$  and  $\delta_e^{18}$ . If the leaf-scale kinetic factors were used, the calculated <sup>18</sup>O-CO<sub>2</sub> isoforcing was severely biased in comparison with the observations. The sensitivity to turbulent diffusion varied over the period shown in Figure 3a. From DOY 207 to 212,  $r_c^c$  increased steadily with time due to the progressive depletion of soil moisture. The highest daytime  $r_c^c$  occurred on DOY 212, with  $r_c^c$  exceeding  $r_a$  by nearly 15-fold. The rain events on DOY 213 and 214

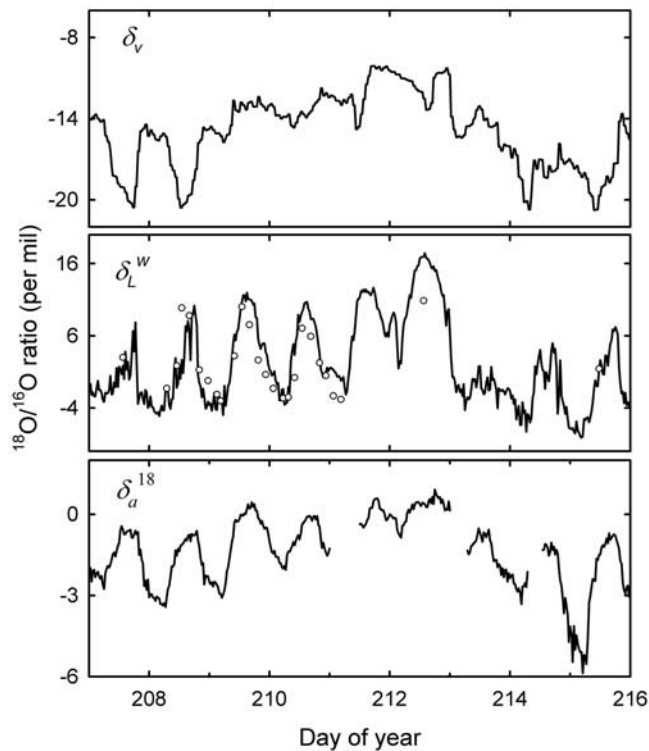


**Figure 2.** Time series of the <sup>18</sup>O compositions of water vapor ( $\delta_v$ ) and CO<sub>2</sub> ( $\delta_a^{18}$ ) in the surface layer and the <sup>18</sup>O composition of the steady state leaf laminar water ( $\delta_L^w$ ) in the soybean canopy. Also shown is the measured <sup>18</sup>O composition of bulk canopy water (open circles, average of upper and lower leaves).

brought  $r_c^e$  down substantially. Ignoring  $r_a$ , as in equations (18) and (19), resulted in large errors when  $r_c^e$  was small. Inclusion of turbulent diffusion, as in equations (15) and (17), significantly improved the comparison.

[33] Figure 3a also suggests a compensating mechanism between the photosynthetic uptake of CO<sub>2</sub> and canopy kinetic fractionation. Higher uptake usually occurred on days when  $r_c^e$  was smaller. On those days, the reduced canopy kinetic fractionation caused smaller isotopic gradient between the stomatal cavity and the air in the surface layer, offsetting the high uptake and resulting in a relatively stable  $C_a(\overline{w'\delta'})^{18}$  from day to day.

[34] Figure 4 shows the diurnal composite of the calculated eddy isoforcing over the main growing season (DOY 190 to 240) when LAI was greater than 2. Outside this period, the various resistance formulae were no longer accurate (see Appendix A). The calculated <sup>18</sup>O-CO<sub>2</sub> eddy isoforcing had a daily peak value of 350  $\mu\text{mol m}^{-2} \text{s}^{-1}$  per mil. This estimate changed to 760  $\mu\text{mol m}^{-2} \text{s}^{-1}$  per mil if turbulent diffusion was ignored, giving a sensitivity of  $\sim 120\%$ . Such sensitivity dwarfed the uncertainties in some biological variables. For example, the photosynthetic isoforcing was parameterized with CO<sub>2</sub> in the intercellular space (equation (21)). Taking into account the drawdown across the mesophyll cell wall with a mesophyll conduc-

tance of 1  $\text{mol m}^{-2} \text{s}^{-1}$  [Gillon and Yakir, 2000a] would reduce the isoforcing by less than 5%.

[35] In comparison, air turbulence had a minor effect on the <sup>13</sup>C-CO<sub>2</sub> isoforcing (Figure 3b), with an average sensitivity of 1.5% at midday. The average midday eddy isoforcing was 580  $\mu\text{mol m}^{-2} \text{s}^{-1}$  per mil over the period DOY 190–240.

[36] Table 1 summarizes the impact of turbulent diffusion on the Craig-Gordon model calculation of the leaf enrichment in <sup>18</sup>O-H<sub>2</sub>O. If the canopy kinetic factor for <sup>18</sup>O-H<sub>2</sub>O was used (equation (17)), the model gave a midday mean  $\delta_L^w$  of 4.5 per mil for the soybean canopy, which was slightly higher (by 0.7 per mil) than the observed <sup>18</sup>O composition of bulk leaf water. Other researchers have also observed similarly small difference between  $\delta_L^w$  and the bulk leaf water  $\delta$  [Gillon and Yakir, 2000b]. If the leaf kinetic factor was used (equation (19)), the model-calculated value was much too high (9.8 per mil). Weighted by the gross CO<sub>2</sub> flux, the calculated  $\delta_L^w$  was 3.2 and 8.3 per mil with the use of the canopy and the leaf kinetic factor, respectively.

[37] There are several reasons why the <sup>18</sup>O-CO<sub>2</sub> isoforcing was much more sensitive to air turbulence than the <sup>13</sup>C-CO<sub>2</sub> isoforcing. In the numerator of equations (15)–(17),

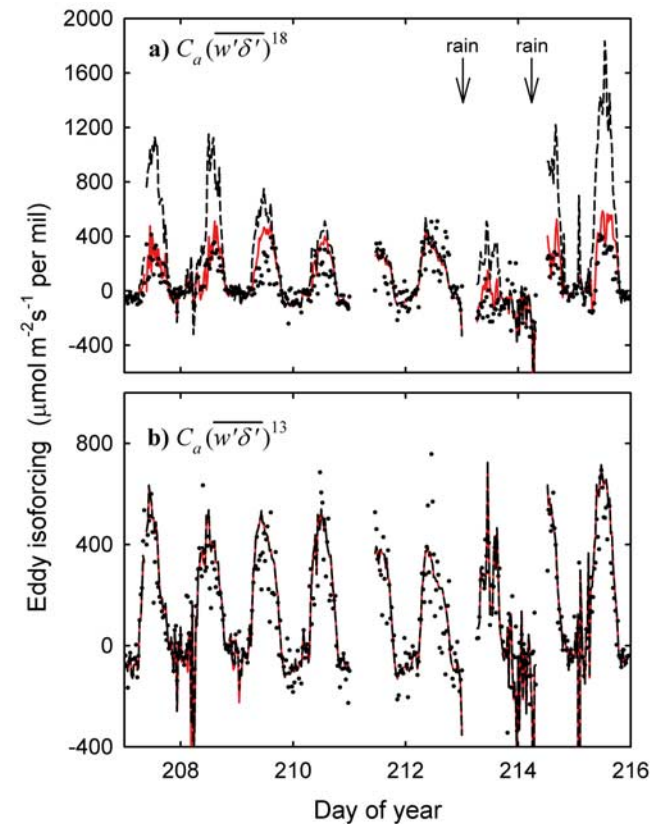


**Figure 3.** Eddy isoforcing over the soybean canopy. (a) Comparison of the observed eddy isoflux of <sup>18</sup>O-CO<sub>2</sub> (dots) with values calculated with the big-leaf parameterization with (solid red line) and without (black dashed line) considering turbulent diffusion. (b) Same as Figure 3a, but for <sup>13</sup>C-CO<sub>2</sub>.

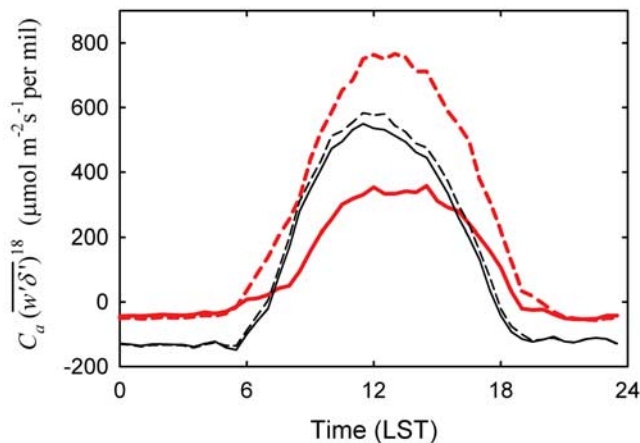


**Figure 4.** Diurnal composite of the eddy isoforcing of <sup>18</sup>O-CO<sub>2</sub> calculated with the big-leaf parameterization. Thick red lines represent the isoforcing calculated for the soybean ecosystem, and thin black lines represent the isoforcing calculated for the forest, with the solid and dashed line shapes corresponding to calculations with and without turbulent diffusion, respectively.

the first term was usually much smaller than the second term. The discrimination of molecular diffusion against <sup>18</sup>O-CO<sub>2</sub> is twice as strong as against <sup>13</sup>C-CO<sub>2</sub>. The same  $r_a$  would result in roughly twice as much reduction in the canopy kinetic factor for <sup>18</sup>O-CO<sub>2</sub> from its molecular value (8.8 per mil) than for <sup>13</sup>C-CO<sub>2</sub> (molecular value 4.4 per mil). The direct effect of turbulence on  $C_a(w'\delta')_c^{18}$ , through the reduction of  $\epsilon_k^{18}$  in equation (21), was, however, rather modest for the soybean ecosystem, typically 80  $\mu\text{mol m}^{-2} \text{s}^{-1}$  per mil in midday, and was not enough to explain the sensitivity in Figure 4. A much larger effect arose, indirectly, through modification of the <sup>18</sup>O-CO<sub>2</sub> isotopic gradient across the stomatal pathway by the <sup>18</sup>O-H<sub>2</sub>O exchange. Of the three isotope species investigated in this study, the kinetic fractionation of <sup>18</sup>O-H<sub>2</sub>O was impacted most by turbulent diffusion, primarily because the smaller stomatal resistance to H<sub>2</sub>O shifted a larger weighting to  $r_a$  when computing the kinetic factor (equations (17) and (A2)). Consequently, the Craig-Gordon model prediction of  $\delta_L^w$  was very sensitive to turbulent diffusion (Table 1). It was the change in  $\delta_L^w$  (and hence  $\delta_e^{18}$ ) that explains most of the sensitivity shown in Figure 4.

[38] The sensitivity can be further understood through the examination of a numerical example (Table 2). Over the 30-min period between 13:00 and 1330 LST on DOY 208, the calculated canopy eddy isoforcing  $C_a(w'\delta')_c^{18}$  and  $C_a(w'\delta')_c^{13}$  were 291 and 422  $\mu\text{mol m}^{-2} \text{s}^{-1}$  per mil, respectively. These estimates changed to 1135 and 429  $\mu\text{mol m}^{-2} \text{s}^{-1}$  per mil, respectively, if the leaf-scale kinetic factors were used. Over 90% of the change in  $C_a(w'\delta')_c^{18}$  was caused by the first term in the square brackets of equation (21) due to the large (11 per mil) increase in the estimate of  $\delta_e^{18}$ . Because of the low canopy resistance in this period, the <sup>18</sup>O-CO<sub>2</sub> isoforcing calculation shows extremely high sensitivity to how the kinetic factors were determined, much more so than the average for the growing season (Figure 4).

[39] To check the consistency of our isoforcing parameterization, in Figure 5 we compare the diurnal patterns of the calculated isoforcing ( $w'\delta'$ ) and the observed isotopic compositions of <sup>13</sup>C-CO<sub>2</sub> and <sup>18</sup>O-CO<sub>2</sub> ( $\delta_a^{13}$  and  $\delta_a^{18}$ ) over the soybean canopy. The daily minimum value of  $\delta_a$  occurred approximately at the time when  $w'\delta'$  changed from being negative to being positive and maximum when  $w'\delta'$  changed from being positive to being negative. Such timing indicates that  $\delta_a$  in the surface layer was tightly controlled by the vegetation-air isotopic exchange. The diurnal amplitude of the <sup>13</sup>C-CO<sub>2</sub> isoforcing was 0.031 per mil  $\text{m s}^{-1}$  or  $\sim 1.4$  times that of the <sup>18</sup>O-CO<sub>2</sub> isoforcing. The isoforcing amplitude ratio was comparable to the ratio of the diurnal amplitudes of the  $\delta_a$  value of <sup>13</sup>C-CO<sub>2</sub> (2.7 per mil) and <sup>18</sup>O-CO<sub>2</sub> (1.8 per mil). These consistent features lend further support to our calculation of the canopy kinetic effects.

[40] Turning attention now to the temperate forest, we note that its surface roughness ( $z_o$ ) was  $\sim 20$  times as large as that of the soybean ecosystem. The kinetic effects of the forest were larger than for the soybean canopy, owing to more vigorous turbulence (smaller  $r_a$ ) which is an important characteristic of air motion in tall vegetation, and higher  $r_c$  (Figure 6). The Craig-Gordon model predicted a higher  $\delta_L^w$  for the forest than for the soybean canopy despite the isotopically lighter atmospheric vapor and the xylem water during the forest experiment (Table 1). No measurement of the leaf water  $\delta$  was available for comparison. But we note that the Craig-Gordon prediction was in the range (7–9 per mil) reported by the MIBA network for temperate forests in the northeastern United States (<http://public.ornl.gov/ameriflux/resource/meetingworkshops.shtml>). The calculated midday  $C_a(w'\delta')_c^{18}$  was 50% higher for the forest than for the soybean canopy even though the forest had a 15% lower rate of CO<sub>2</sub> uptake. The forest isoforcing was less sensitive to turbulent diffusion than that of the soybean canopy, increasing by 6% at midday if  $r_a$  was excluded from the calculation of the kinetic factors.

[41] Figure 6 presents the diurnal composites of the three kinetic factors in the soybean and the forest canopy. Of the three isotopologues, <sup>18</sup>O-H<sub>2</sub>O displayed the largest diurnal variations in its kinetic factor. The canopy resistance inferred from the Penman-Monteith equation had average

**Table 1.** Growing Season Mean <sup>18</sup>O-H<sub>2</sub>O Composition of Leaf Water<sup>a</sup>

|         | Midday (1200–1500 LST) |                  |                  | Weighted by Gross CO <sub>2</sub> Flux |                  |
|---------|------------------------|------------------|------------------|--|------------------|
|         | $\delta_{L,b}^w$       | $\delta_{L,1}^w$ | $\delta_{L,2}^w$ | $\delta_{L,1}^w$                       | $\delta_{L,2}^w$ |
| Soybean | 3.8                    | 4.5              | 9.8              | 3.3                                    | 8.3              |
| Forest  | NA                     | 8.3              | 8.9              | 9.2                                    | 9.8              |

<sup>a</sup>Composition per mil, referenced to the VSMOW scale. Abbreviations are as follows:  $\delta_{L,b}^w$ , measured bulk leaf water (average of upper and lower leaves in the canopy);  $\delta_{L,1}^w$  and  $\delta_{L,2}^w$ , Craig-Gordon prediction with and without turbulent diffusion, respectively; NA, not applicable. The <sup>18</sup>O compositions of atmospheric vapor and xylem water were  $-15.7$  and  $-7.6$  per mil in the soybean ecosystem and  $-17.2$  and  $-9.1$  per mil in the forest, respectively.

**Table 2.** Sensitivity Analysis for Period 1300–1330 LST, DOY 208<sup>a</sup>

|                | $\epsilon_k^w$<br>(per mil) | $\epsilon_k^{18}$<br>(per mil) | $\epsilon_k^{13}$<br>(per mil) | $\delta_L^w$<br>(per mil) | $\delta_e^{18}$<br>(per mil) | $C_a(\overline{w'\delta'})_e^{18}$<br>( $\mu\text{mol m}^{-2}\text{s}^{-1}$ per mil) | $C_a(\overline{w'\delta'})_e^{13}$<br>( $\mu\text{mol m}^{-2}\text{s}^{-1}$ per mil) |
|----------------|-----------------------------|--------------------------------|--------------------------------|---------------------------|------------------------------|--|--|
| $r_a$ included | 9.1                         | 3.3                            | 1.7                            | 2.3                       | 2.4                          | 291  | 422  |
| $r_a$ excluded | 28.2                        | 7.9                            | 3.9                            | 13.7                      | 13.4                         | 1135   | 429  |

<sup>a</sup>Variable definitions are provided in the notation section. In this period, the values of the intermediate variables are as follows:  $r_a = 79 \text{ s m}^{-1}$ ;  $r_b^w = 13 \text{ s m}^{-1}$ ;  $r_c^w = 25 \text{ s m}^{-1}$ ;  $C_a = 369.0 \text{ ppm}$  ( $15,240 \mu\text{mol m}^{-3}$ );  $C = 308.5 \text{ ppm}$  ( $12,740 \mu\text{mol m}^{-3}$ );  $F_c = -18.5 \mu\text{mol m}^{-2}\text{s}^{-1}$ ;  $\delta_a^{18} = -1.1 \text{ per mil}$ ;  $\delta_a^{13} = -7.9 \text{ per mil}$ .

values of 53 and  $120 \text{ s m}^{-1}$  in midafternoon (1200–1500 LST) and 450 and  $1800 \text{ s m}^{-1}$  at night (2300–0200 LST) in the soybean and the forest ecosystem, respectively. The midafternoon values were higher than the minimum values of 30 and  $50 \text{ s m}^{-1}$  reported for agricultural crops and natural vegetation, respectively [Kelliher *et al.*, 1995]. Since gaseous diffusion through the stomatal opening is purely a molecular process, the large diurnal change in the canopy resistance is one reason explaining the diurnal patterns shown in Figure 6. The kinetic factors weighted by the gross CO<sub>2</sub> flux were 28.6, 8.1 and 4.0 per mil in the forest and 16.8, 4.2, 2.1 per mil in the soybean ecosystem for <sup>18</sup>O-H<sub>2</sub>O, <sup>18</sup>O-CO<sub>2</sub> and <sup>13</sup>C-CO<sub>2</sub>, respectively. For comparison, the molecular values of the kinetic factors are 32, 8.8 and 4.4, respectively. Ogée *et al.* [2003] used a mean value of  $\epsilon_k^{13} = 3.6 \text{ per mil}$  in their investigation of flux partitioning in a forest.

[42] Figure 7 presents a comparison of the dependence of the kinetic factor for <sup>18</sup>O-H<sub>2</sub>O ( $\epsilon_k^w$ ) on wind speed among three surface types in neutral stability. The result of Merlivat and Jouzel [1979] has been updated with the molecular value of Cappa *et al.* [2003]. In typical wind conditions encountered on land,  $\epsilon_k^w$  of the two ecosystems was quite sensitive to wind speed, increasing by 10 per mil in the soybean and 7 per mil in the forest as wind speed increased from 1 to  $4 \text{ m s}^{-1}$ . In comparison, the kinetic factor of the water surface is much less sensitive, changing by about 1 per mil over the same wind speed range.

## 5. Discussion

### 5.1. Kinetic Fractionation in Different Reference Frames

[43] Our analysis suggests that the extent of kinetic fractionation should be dependent upon the frame of reference used for measurement or modeling. The leaf-scale formulation is desired if variables, such as  $\delta_a$ ,  $C_a$ ,  $\delta_v$ ,  $T_a$  and  $u$  that are used as inputs to predict the isotopic fluxes, are measured immediately outside the leaf boundary layer, as in most chamber-based studies. In the canopy framework, because these input variables are all measured in the surface layer over the canopy, the canopy-scale kinetic factors are preferred. We suggest that use of the canopy-scale kinetic factors may bring improvement to the calculation of isotopic budgets in regional and global modeling studies [Hoffmann *et al.*, 2004; Cuntz *et al.*, 2003; Kaplan *et al.*, 2002; Ciais *et al.*, 1995, 1997; Lloyd and Farquhar, 1994; Farquhar *et al.*, 1993] and to the estimation of biome-specific discrimination factors using either observed or model-derived meteorology

[Randerson *et al.*, 2002; Gillon and Yakir, 2001; Lloyd and Farquhar, 1994; Farquhar *et al.*, 1993]. Common to these two types of research is that prognostic variables in the atmospheric boundary layer are used as inputs to drive the parameterization of land-atmosphere interactions.

[44] Numerous investigators have quantified leaf water enrichment in <sup>18</sup>O-H<sub>2</sub>O in field conditions [e.g., Seibt *et al.*, 2007; Lai *et al.*, 2005; Cernusak *et al.*, 2002; Harwood *et al.*, 1999; Flanagan *et al.*, 1997]. Because relative humidity and  $\delta_v$ , two critical inputs required by the Craig-Gordon model, are accurately measured inside the canopy, the role of turbulence in kinetic fractionation should be minimal. Likewise from a modeling perspective, if these variables are solved for the airspace inside the canopy, as in the two-leaf model of Riley *et al.* [2002], the leaf-scale factors should provide an accurate prediction of the kinetic effects. Multilayer models such as CANISOTOPE and MuSICA are also capable of resolving the within-canopy prognostic variables [Ogée *et al.*, 2003; Baldocchi and Bowling, 2003].

[45] The study of Cappa *et al.* [2003] appears to be an exception. In their chamber study of isotopic fractionation of water during evaporation, the evaporating dish has a dimension of 6.6 cm and can be considered a good physical analogue of a leaf. Their kinetic effect is described by  $n = 0.35$ , not 2/3 as expected for a laminar boundary layer. This raises the possibility that even in a well-mixed chamber, turbulent diffusion may still play a role.

### 5.2. GPP-Weighted Kinetic Factors

[46] Lloyd and Farquhar [1994] estimated GPP (gross primary production) for the major biome types of the world. Assuming that our  $\epsilon_k$  values for the temperate forest and the soybean ecosystem were typical of the global forest biomes and biomes of short stature (cropland, grassland, tundra), respectively, we arrived at GPP-weighted  $\epsilon_k$  values of 24.5, 6.8 and 3.5 per mil for <sup>18</sup>O-H<sub>2</sub>O, <sup>18</sup>O-CO<sub>2</sub> and <sup>13</sup>C-CO<sub>2</sub>, respectively. Our estimate for <sup>18</sup>O-H<sub>2</sub>O would be lower if we used the molecular value reported by Merlivat [1978] instead of Cappa *et al.* [2003]. Such extrapolation is obviously very crude but nevertheless serves as a basis for comparison with the kinetic factors used in the published studies of global isotopic budgets [Hoffmann *et al.*, 2004; Cuntz *et al.*, 2003; Kaplan *et al.*, 2002; Ciais *et al.*, 1995, 1997; Lloyd and Farquhar, 1994; Farquhar *et al.*, 1993]. In these studies,  $\epsilon_k^w$  varies from 26.0 to 26.3 per mil,  $\epsilon_k^{18}$  varies from 7.4 to 8.8 per mil, and  $\epsilon_k^{13}$  takes the molecular value of 4.4 per mil. Once again, for the reasons discussed in section 4, the largest difference is seen in <sup>18</sup>O-H<sub>2</sub>O. In a parameter sensitivity analysis, Peylin *et al.* [1996] showed that  $\epsilon_k^{18}$  and

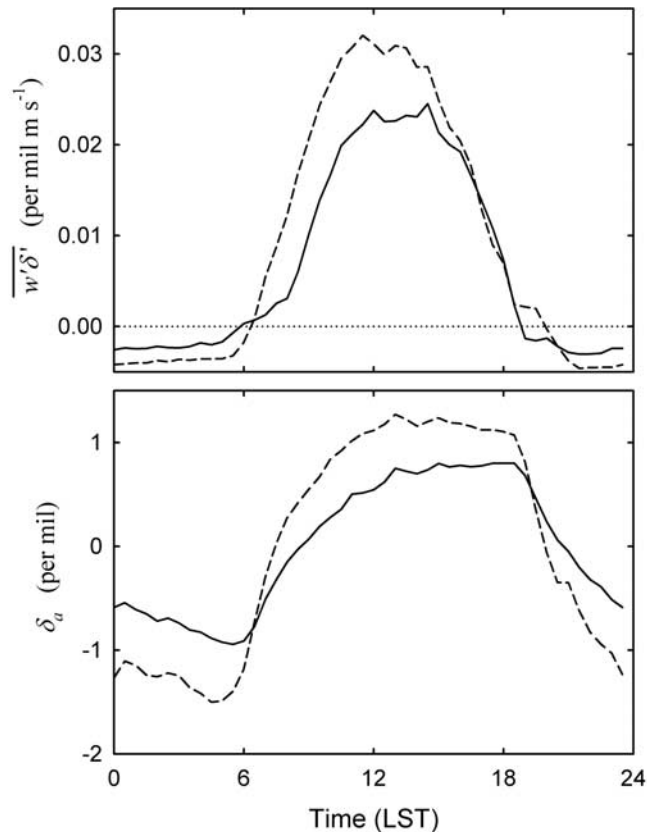


**Figure 5.** Diurnal composite of the calculated isoforcing (top) and isotopic composition of CO<sub>2</sub> (bottom) over the soybean canopy (solid line, <sup>18</sup>O-CO<sub>2</sub>; dashed line, <sup>13</sup>C-CO<sub>2</sub>). The mean  $\delta_a^{18}$  and  $\delta_a^{13}$  values are  $-1.2$  and  $-8.5$  per mil, respectively, for the period DOY 190–240 and have been removed before computing the composites in the bottom panel.

$\epsilon_k^{18}$  optimized for the global <sup>18</sup>O-CO<sub>2</sub> budget are irreconcilable with those for its interhemispheric gradient. Adding  $\epsilon_k^w$  as a third tunable parameter may help eliminate the inconsistency.

[47] Photosynthetic discrimination against <sup>13</sup>C,  $\Delta$ , is a critical parameter in the inference of the land C uptake from <sup>13</sup>C-CO<sub>2</sub> measurements. Using the  $C/C_a$  ratio of Lloyd and Farquhar [1994], we estimated that  $\Delta$  of C<sub>3</sub> plants was 0.33–0.66 per mil lower using the above GPP-weighted  $\epsilon_k^{13}$  than using the molecular  $\epsilon_k^{13}$  value. Ciais *et al.* [1995] showed that a 1 per mil error in  $\Delta$  results in a small error of 0.2 GtC in the carbon sink estimate for the 30°N–90°N latitudinal band. So the impact of turbulence on the inverse C flux calculation is probably limited, consistent with the ecosystem-scale isoforcing sensitivity analysis (Figure 3).

### 5.3. Role of Surface Roughness and Wind

[48] Intuitively, air turbulence, being nondiscriminative in diffusing materials, should act to erase the kinetic effect [Dongmann *et al.*, 1974]. Our results show just the opposite,

that in the terrestrial environment, air turbulence enhances the effect rather than suppressing it. Over a smooth water surface, the effect of air turbulence is to reduce the thickness of the interfacial air layer at the surface where molecular diffusion takes place, therefore weakening the kinetic fractionation on evaporation (Figure 7). The opposite is true on land according to equations (15)–(17). As the level of turbulence increases, the stomatal pathway becomes more limiting to gaseous diffusion, giving rise to stronger kinetic effects. The highest kinetic fractionation is attained when turbulence is infinitely strong, or  $r_a$  (and  $r_b$ )  $\rightarrow 0$ .

[49] According to our analysis, the kinetic effects should be lower in ecosystems of short stature owing to their smaller surface roughness, such as cropland and grassland, than in forest ecosystems (Figures 6 and 7). This leads to several interesting deductions. Under similar hydrological conditions, leaves in cropland and grassland should be less enriched in <sup>18</sup>O-H<sub>2</sub>O than those in forests (Table 1). Conversion of forests to cropland and grassland is likely to change the global coverage of C<sub>4</sub> vegetation, which has a much lower  $\theta_{eq}$  than C<sub>3</sub> plants and thus has the potential to alter the atmospheric budget of <sup>18</sup>O-CO<sub>2</sub> [Gillon and Yakir, 2001]. The effect of land use could be further intensified by the canopy fractionation mechanism, namely the reduction in  $\epsilon_k^{18}$  and in leaf water enrichment in <sup>18</sup>O. The contrasting diurnal patterns of the <sup>18</sup>O-CO<sub>2</sub> isoforcing between the

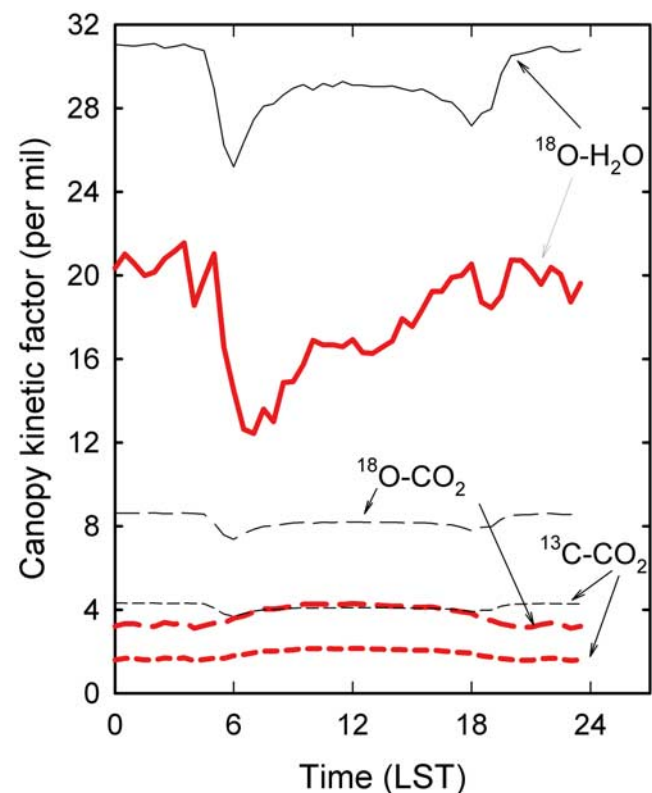


**Figure 6.** Diurnal composite of the canopy-scale kinetic fractionation factors. Thick red lines represent values for the soybean ecosystem, and thin black lines represent values for the forest.

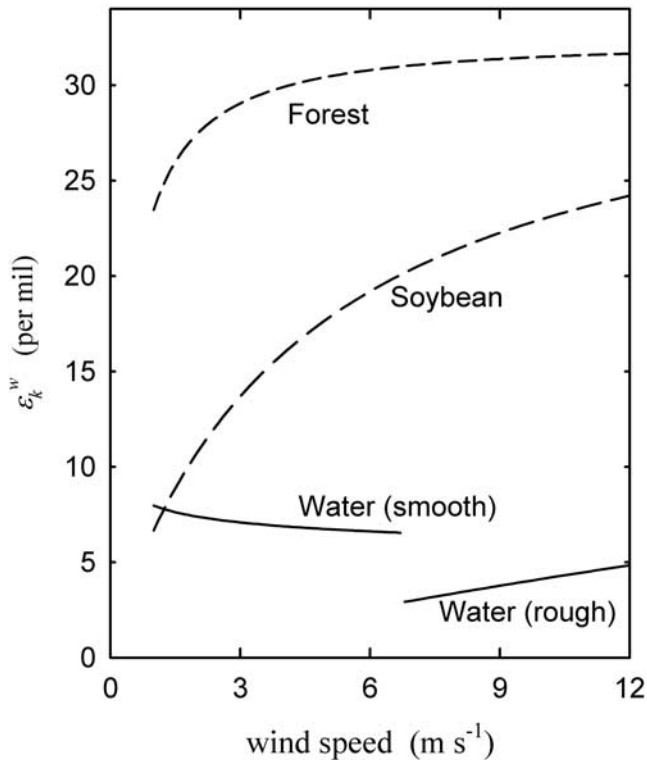


**Figure 7.** Wind dependence of the <sup>18</sup>O-H<sub>2</sub>O kinetic factor for three surface types in neutral stability. The kinetic factors of the soybean and the forest ecosystem are calculated with the mean midafternoon canopy resistance  $r_c^w$  of 54 and 120 s m<sup>-1</sup>, respectively. The kinetic factor for the water surface is given by Merlivat and Jouzel [1979] and is updated with the molecular fractionation value of Cappa et al. [2003].

soybean and the forest (Figure 4) suggest that  $\delta_a^{18}$  should vary more diurnally (and possibly seasonally as well) in a forested landscape than in areas covered by low vegetation. The validity of these deductions is not known at present and will be investigated in our future experimental campaigns.

[50] One conclusion of this study is that the kinetic factors are wind-dependent properties. It is estimated that the surface wind on land declined by ~4% per decade from 1971 to about 2000 [Roderick et al., 2007]. Our sensitivity analysis shows that a 4% reduction in wind speed will decrease  $\epsilon_k^{18}$  and  $\delta_L^w$  by 0.03 and 0.07 per mil, respectively, in the forest and 0.1 and 0.2 per mil, respectively, in the soybean ecosystem. According to the equilibrium solution of Cuntz et al. [2003], these changes are capable of reducing the global  $\delta_a^{18}$  by 0.05–0.2 per mil, which represents a moderate portion of the ~0.5 per mil decrease in  $\delta_a^{18}$  observed in Mauna Loa from 1990 to 1999 by the NOAA flask network. The declining trend in the <sup>18</sup>O-CO<sub>2</sub> record was reversed around 1999. Interestingly, at about the same time reversal of the wind speed trend also occurred in India and Eurasia [Dai, 2007]. It is likely that wind speed is one

of several agents of change including land use [Gillon and Yakir, 2001] and atmospheric humidity [Willett et al., 2007; Santer et al., 2007] contributing to the interannual variability in the <sup>18</sup>O composition of atmospheric CO<sub>2</sub>.

#### 5.4. Leaf Boundary Layer Resistance Versus Excess Resistance

[51] There is no unique treatment of the kinetic effects for diffusion through the interfacial air layer overlaying the surface that exchanges gases with the atmosphere. In the marine environment, kinetic fractionation in the interfacial layer depends on the roughness of the evaporating surface, with the exponent  $n$  in equation (9) varying from 2/3 in the smooth regime to 1/2 in the rough regime according to Brutsaert [1975]. The reader is reminded that the actual kinetic factor is equal to  $n$  times the molecular value (equation (10)). Brutsaert's theory of the rough regime is based on the notion that the transfer in the interfacial layer is accomplished by molecular diffusion into eddies of the size of the Kolmogorov scale that come down randomly in contact with the surface. Since vegetation stands are rough surfaces, it seems that in the interfacial layer of the canopy the kinetic fractionation should be dictated by  $n = 1/2$  [Dongmann et al., 1974]. However, because air motion in a canopy space is turbulent all the time and the eddies that sweep into the canopy occur at scales much greater than the Kolmogorov scale [Denmead and Bradley, 1985], Brutsaert's theory strictly does not hold in the canopy environment. On the basis of the classic theory of boundary layer flow, Farquhar and Lloyd [1993] proposed that the interfacial resistance should fractionate the diffusion process according to  $n = 2/3$ . This  $n$  value agrees with theory on the deposition of pollutants to vegetation surfaces [Lamaud et al., 1994; Fuentes et al., 1992; Wesely and Hicks, 1877].

[52] The total resistance in air ( $r_t$ ) is the sum of a turbulent component ( $r_a$ ), termed aerodynamic resistance, for diffusion above the interfacial layer and an interfacial resistance for diffusion in the interfacial layer. The aerodynamic resistance is independent of molecular diffusivity and therefore nondiscriminating. The standard equation for  $r_t$  (equation (A1); see Appendix A) worked reasonably well for the closed soybean canopy (Figure 8). How to split  $r_t$  into  $r_a$  and the interfacial resistance remains an open question. In the present study, we have used a bulk leaf boundary layer resistance  $r_b$  (equation (A3); see Appendix A) as the interfacial resistance, consistent with the leaf-scale study of Farquhar and Lloyd [1993; see also Bowling et al., 2001; Magnani et al., 1998], and have computed  $r_a$  as the difference between  $r_t$  and  $r_b$  (equation (A4)). An alternative approach is that of Merlivat and Jouzel [1979] who used the excess resistance  $r_e$  to characterize the transfer in the interfacial layer. In neutral stability,  $r_e$  is exclusively the result of different surface roughness for water vapor and momentum [Garratt, 1992]. In stratified air, its physical meaning is rather ambiguous because the difference can also result from the turbulent Prandtl number being different from unity. Using  $r_e$  [Garratt, 1992, equations 3.42 and 3.61] instead of  $r_b$  for the interfacial layer would increase the estimate of <sup>18</sup>O-CO<sub>2</sub> isoforcing by 20% over the soybean

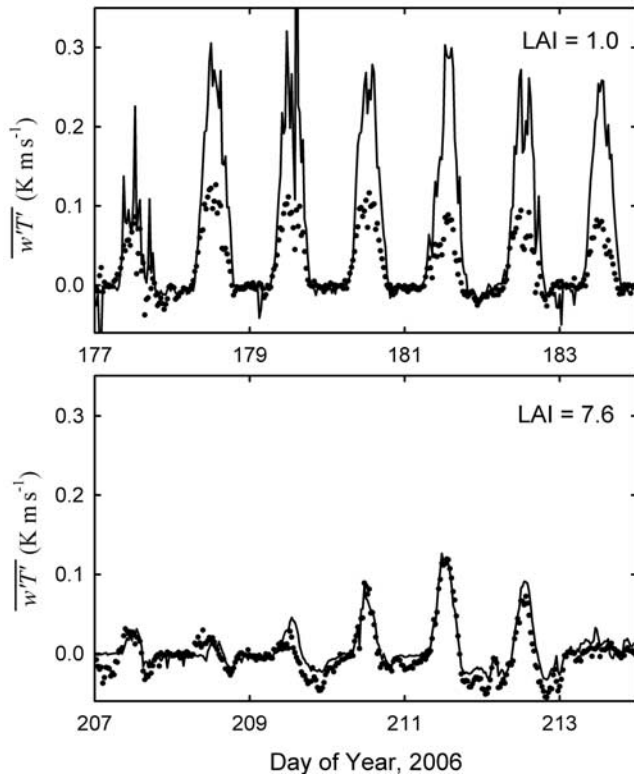


**Figure 8.** Comparison of observed (dots) and calculated sensible heat flux over the soybean canopy. The calculation is made according to  $\overline{wT'} = (T_c - T_a)/r_t$ .

canopy, worsening the comparison against the observed isoforcing.

## 6. Conclusions

[53] The canopy-scale kinetic fractionation is a balancing act between the physical property of air motion and the stomatal control on gaseous exchange. At a given stomatal resistance, the kinetic factors of <sup>13</sup>C-CO<sub>2</sub>, <sup>18</sup>O-CO<sub>2</sub> and <sup>18</sup>O-H<sub>2</sub>O increase with increasing wind speed, surface roughness or both. Of the three isotopologues investigated, the kinetic factor of <sup>18</sup>O-H<sub>2</sub>O is most sensitive to turbulent diffusion and that of <sup>13</sup>C-CO<sub>2</sub> least. The sensitivity to turbulence is particularly striking in situations where the canopy resistance is low in comparison to the aerodynamic resistance. The canopy-scale kinetic factors are more appropriate than the leaf-scale values for the determination of isotopic gaseous exchange where input variables are provided, either by observations or by model calculations, at a reference point outside the canopy airspace.

[54] Ignoring turbulent diffusion can cause large errors in the predictions of vegetation-air isotopic exchange. In the soybean ecosystem, use of the leaf kinetic factors increase the estimates of seasonal mean leaf isotopic content by 5.0 per mil, the whole-ecosystem <sup>18</sup>O-CO<sub>2</sub> isoforcing on the atmosphere by 120% and the <sup>13</sup>C-CO<sub>2</sub> isoforcing by 1.5%. In the forest ecosystem, because of a higher

canopy resistance, these estimates are less sensitive to turbulent diffusion.

[55] The canopy fractionation mechanism can contribute to the spatial and temporal variations in atmospheric <sup>18</sup>O-CO<sub>2</sub> ( $\delta_a^{18}$ ). The dependence on surface roughness suggests that  $\delta_a^{18}$  should vary more diurnally in a forested landscape than in areas covered by low vegetation. Similarly, higher wind conditions should create stronger kinetic effects therefore enriching the air with <sup>18</sup>O-CO<sub>2</sub>. It is known that atmospheric <sup>18</sup>O-CO<sub>2</sub> is tightly linked to the hydrological cycle. Our research shows that it is also linked to the wind circulation on land. We postulate that temporal trends in wind speed are an agent of change contributing to the interannual variability in global  $\delta_a^{18}$ .

## Appendix A: Computation of Resistance Terms

[56] All the resistance terms are determined with standard procedures found in the LSM literature. A typical soil resistance value for H<sub>2</sub>O is [Shuttleworth and Gurney, 1990]

$$r_s^w = 500 \text{ s m}^{-1}.$$

In our calculations, we assume the soil resistance for CO<sub>2</sub> is

$$r_s^c = 1.6 \times 500 = 800 \text{ s m}^{-1}.$$

[57] The total resistance to heat and water vapor between the foliar surface and the reference height  $z_m$  above the canopy is given by

$$r_t = 1/(u_m C_H), \quad (\text{A1})$$

where the transfer coefficient is [Garratt, 1992]

$$C_H = k^2 / \{ [\ln((z_m - d)/z_o) - \Phi_m] [\ln((z_m - d)/z_q) - \Phi_h] \},$$

where  $u_m$  is wind speed at the reference height  $z_m$  ( $= 3.0$  m for the soybean ecosystem and  $30.4$  m for the forest),  $k$  is the von Karman constant,  $d$  is displacement height,  $z_o$  and  $z_q$  are momentum and humidity roughness, respectively, and  $\Phi_m$  and  $\Phi_h$  are the integral Monin-Obukhov similarity functions for momentum and heat, respectively. The aerodynamic parameters are given by

$$d = 0.7h; \quad z_o = 0.1h; \quad z_q = z_o / \exp(kB^{-1}),$$

where  $h$  is canopy height and  $B^{-1}$  is the inverse of the Dalton number of the interfacial sublayer. For vegetation canopy, an average value of  $B^{-1}$  is [Garratt, 1992]

$$B^{-1} = 2/k.$$

Grace *et al.* [1995] reported that the canopy resistance inferred from the Penman-Monteith equation is sensitive to the choice of  $B^{-1}$ . In the present study, with the average value recommended by Garratt [1992], the resistance formulation gives good prediction of the sensible heat flux

during the period with leaf area index  $L > 2$ . Outside the period, the predicted heat flux is not accurate (Figure 8).

[58] The canopy resistance to H<sub>2</sub>O,  $r_c^w$ , is determined with the Penman-Monteith equation using the measured vapor density deficit ( $D$ ),  $r_t$ , and sensible heat ( $w'T'$ ) and water vapor flux ( $w'\rho'_v$ )

$$r_c^w = \frac{D}{w'\rho'_v} + r_t \left( \frac{w'T'}{w'\rho'_v} s - 1 \right),$$

where the slope of the saturation vapor density curve,  $s$  is evaluated at air temperature. The canopy resistance to CO<sub>2</sub> is given by

$$r_c^c = 1.6 r_c^w. \quad (\text{A2})$$

The Penman-Monteith equation is not accurate in a sparse canopy where soil evaporation makes a large contribution to the whole ecosystem latent heat flux [Kelliher et al., 1995; Shuttleworth and Gurney, 1990]. In this study, the isoforcing computation is limited to the periods when  $L$  was greater than 2 in the soybean experiment (DOY 190–240) and when the trees were fully leafed in the forest experiment (DOY 150–260).

[59] Dew formation was a commonplace at both field sites at night. In dew events, the water vapor flux over the canopy would become negative, and the calculated  $r_c$  would be unreasonably small or even negative. To remove the dew interference, we assigned default values to  $r_c$  when the water vapor flux was negative. These default values were determined from the average nighttime  $r_c$  calculated in dew-free conditions. They varied from 500 s m<sup>-1</sup> at  $L = 2$  to 300 s m<sup>-1</sup> at  $L = 8$  in the soybean experiment and were 2000 s m<sup>-1</sup> in the forest experiment.

[60] To determine the leaf boundary layer resistance, we assume that the wind speed inside the canopy takes the usual exponential form whose extinction coefficient is controlled by  $L$ , as [Lee, 2000]

$$a = -0.030L^2 + 0.66L + 0.70.$$

The mean wind speed inside the canopy,  $u_c$ , is [Baldocchi, 1988]

$$u_c = \frac{u_h}{a} [1 - \exp(-a)]$$

$$u_h = u_m \ln[(h - d)/z_o] / \ln[(z_m - d)/z_o].$$

The leaf boundary layer resistance to H<sub>2</sub>O, scaled to the canopy, is given by [Campbell, 1977; Shuttleworth and Gurney, 1990]

$$r_b^w = \frac{b}{2L} \left( \frac{L_w}{u_c} \right)^{0.5}, \quad (\text{A3})$$

where  $b = 283 \text{ s}^{0.5} \text{ m}^{-1}$  and  $L_w$  is leaf dimension (= 0.05 m). The boundary layer resistance to CO<sub>2</sub> is related to  $r_b^w$  as

$$r_b^c = 1.4 r_b^w.$$

[61] The aerodynamic resistance in the surface layer is nondiscriminating. It is computed as the difference between  $r_t$  and  $r_b^w$

$$r_a = r_t - r_b^w. \quad (\text{A4})$$

[62] The aerodynamic resistance between the soil surface and the top of the canopy, also nondiscriminating, is found by integrating the reciprocal of the eddy diffusivity  $K$  as [Baldocchi, 1988]

$$r_{a,s} = \int_0^h \frac{dz}{K}.$$

Here  $K$  is determined with the procedure described by Lee [2003] on the basis of the near-field Lagrangian theory [Raupach, 1989]. The <sup>18</sup>O-CO<sub>2</sub> isoforcing is not sensitive to  $r_{a,s}$ , changing by less than 2% with a  $\pm 50\%$  change in  $r_{a,s}$ .

## Notation

|                       |  |
|-----------------------|--|
| $( )^{18}$            | <sup>18</sup> O-CO <sub>2</sub> .  |
| $( )^{13}$            | <sup>13</sup> C-CO <sub>2</sub> .  |
| $( )^c$               | CO <sub>2</sub> .  |
| $( )^w$               | H <sub>2</sub> O.  |
| $( )_a$               | air.   |
| $( )_c$               | canopy.  |
| $( )_i$               | minor isotopic species of CO <sub>2</sub> .  |
| $( )_s$               | soil.  |
| $( )$                 | temporal averaging operator.   |
| $( )'$                | deviation from temporal average.   |
| $\delta$              | isotope ratio in delta notation (per mil).   |
| $\delta_a^{13}$       | <sup>13</sup> C-CO <sub>2</sub> $\delta$ at height $z_m$ (per mil).                        |
| $\delta_a^{18}$       | <sup>18</sup> O-CO <sub>2</sub> $\delta$ at height $z_m$ (per mil).                        |
| $\delta_{L,b}^w$      | <sup>18</sup> O-H <sub>2</sub> O $\delta$ of bulk leaf water (per mil).                    |
| $\delta_L^w$          | Craig-Gordon prediction <sup>18</sup> O-H <sub>2</sub> O $\delta$ of leaf water (per mil). |
| $\delta_e^{18}$       | <sup>18</sup> O-CO <sub>2</sub> $\delta$ in equilibrium with laminar leaf water (per mil). |
| $\delta_v$            | <sup>18</sup> O-H <sub>2</sub> O $\delta$ of atmospheric vapor (per mil).                  |
| $\delta_F$            | flux isotope ratio in delta notation (per mil).  |
| $\delta_R^{13}$       | <sup>13</sup> C-CO <sub>2</sub> $\delta$ of soil respiration (per mil).                    |
| $\epsilon_k^{13}$     | canopy kinetic fractionation factor for <sup>13</sup> C-CO <sub>2</sub> (per mil).         |
| $\epsilon_{k,s}^{18}$ | soil kinetic fractionation factor for <sup>18</sup> O-CO <sub>2</sub> (per mil).           |
| $\epsilon_k^{18}$     | canopy kinetic fractionation factor for <sup>18</sup> O-CO <sub>2</sub> (per mil).         |
| $\epsilon_k^w$        | canopy kinetic fractionation factor for <sup>18</sup> O-H <sub>2</sub> O (per mil).        |
| $\theta_{eq}$         | extent of CO <sub>2</sub> hydration in leaves.   |
| $\Phi_h$              | integral similarity function for heat.   |
| $\Phi_m$              | integral similarity function for momentum.   |

|                                  |  |
|----------------------------------|--|
| <i>a</i>                         | extinction coefficient of the within-canopy wind profile.  |
| <i>b</i>                         | boundary layer resistance coefficient ( $s^{0.5} m^{-1}$ ).  |
| <i>b</i>                         | <sup>13</sup> C discrimination factor in the carboxylation reaction (per mil).                             |
| <i>c</i>                         | CO <sub>2</sub> mixing ratio ( $\mu\text{mol mol}^{-1}$ ).   |
| <i>C</i>                         | CO <sub>2</sub> molar concentration in the intercellular space ( $\mu\text{mol m}^{-3}$ ).                 |
| <i>C<sub>a</sub></i>             | CO <sub>2</sub> molar concentration at height <i>z<sub>m</sub></i> ( $\mu\text{mol m}^{-3}$ ).             |
| <i>C<sub>s</sub></i>             | CO <sub>2</sub> molar concentration in soil air ( $\mu\text{mol m}^{-3}$ ).                                |
| <i>C<sub>H</sub></i>             | transfer coefficient.  |
| <i>d</i>                         | displacement height (m).   |
| <i>F</i>                         | whole-ecosystem CO <sub>2</sub> flux ( $\mu\text{mol m}^{-2}\text{s}^{-1}$ ).                              |
| <i>F<sub>c</sub></i>             | canopy CO <sub>2</sub> flux ( $\mu\text{mol m}^{-2}\text{s}^{-1}$ ).                                       |
| <i>F<sub>s</sub></i>             | soil CO <sub>2</sub> flux ( $\mu\text{mol m}^{-2}\text{s}^{-1}$ ).   |
| <i>h</i>                         | canopy height (m).   |
| <i>K</i>                         | eddy diffusivity ( $\text{m}^2 \text{s}^{-1}$ ).   |
| <i>k</i>                         | resistance ratio; von Karman constant.   |
| <i>L</i>                         | leaf area index.   |
| <i>l<sub>w</sub></i>             | leaf dimension (m).  |
| <i>r<sub>a</sub></i>             | aerodynamic resistance in the surface layer ( $\text{s m}^{-1}$ , $\text{m}^2 \text{s mol}^{-1}$ ).        |
| <i>r<sub>a,s</sub></i>           | aerodynamic resistance in the canopy air layer ( $\text{s m}^{-1}$ , $\text{m}^2 \text{s mol}^{-1}$ ).     |
| <i>r<sub>b</sub><sup>c</sup></i> | leaf boundary layer resistance to CO <sub>2</sub> ( $\text{s m}^{-1}$ , $\text{m}^2 \text{s mol}^{-1}$ ).  |
| <i>r<sub>c</sub><sup>c</sup></i> | canopy resistance to CO <sub>2</sub> ( $\text{s m}^{-1}$ , $\text{m}^2 \text{s mol}^{-1}$ ).               |
| <i>r<sub>s</sub><sup>c</sup></i> | soil resistance to CO <sub>2</sub> ( $\text{s m}^{-1}$ , $\text{m}^2 \text{s mol}^{-1}$ ).                 |
| <i>r<sub>t</sub></i>             | total resistance above the foliage surface ( $\text{s m}^{-1}$ , $\text{m}^2 \text{s mol}^{-1}$ ).         |
| <i>r<sub>b</sub><sup>w</sup></i> | leaf boundary layer resistance to H <sub>2</sub> O ( $\text{s m}^{-1}$ , $\text{m}^2 \text{s mol}^{-1}$ ). |
| <i>r<sub>c</sub><sup>w</sup></i> | canopy resistance to H <sub>2</sub> O ( $\text{s m}^{-1}$ , $\text{m}^2 \text{s mol}^{-1}$ ).              |
| <i>R</i>                         | CO <sub>2</sub> molar isotope ratio.   |
| <i>R<sub>a</sub></i>             | CO <sub>2</sub> molar isotope ratio at height <i>z<sub>m</sub></i> .                                       |
| <i>R<sub>e</sub></i>             | molar isotope ratio of CO <sub>2</sub> in equilibrium with leaf laminar water.                             |
| <i>t</i>                         | time.  |
| <i>T<sub>a</sub></i>             | air temperature (°C).  |
| <i>T<sub>c</sub></i>             | canopy temperature (°C).   |
| <i>u, v, w</i>                   | velocity components in the { <i>x, y, z</i> } direction ( $\text{m s}^{-1}$ ).                             |
| <i>u<sub>c</sub></i>             | mean wind speed in the canopy ( $\text{m s}^{-1}$ ).   |
| <i>u<sub>h</sub></i>             | wind speed at the canopy top ( $\text{m s}^{-1}$ ).  |
| <i>u<sub>m</sub></i>             | wind speed at reference height ( $\text{m s}^{-1}$ ).  |
| <i>x, y, z</i>                   | coordinate in the longitudinal, lateral, and vertical direction.   |
| <i>z<sub>m</sub></i>             | reference height in the surface layer (m).   |
| <i>z<sub>o</sub></i>             | surface roughness for momentum (m).  |
| $\frac{z_q}{z_o}$                | surface roughness for humidity (m).  |
| $\frac{w'\delta'}{w'\delta'}$    | isoforcing (per mil $\text{m s}^{-1}$ ).   |
| $C_a(w'\delta')$                 | eddy isoforcing ( $\mu\text{mol m}^{-2}\text{s}^{-1}$ per mil).  |
| $\frac{w'T'}{w'\rho'}$           | kinematic sensible heat flux ( $\text{K m s}^{-1}$ ).  |
| $\frac{w'\rho'}{w'\rho'}$        | water vapor flux ( $\text{g m}^{-2}\text{s}^{-1}$ ).   |

[63] **Acknowledgments.** This work was supported by the U.S. National Science Foundation (grants ATM-0546476, DEB-0514908, DEB-0514904, EAR-0229343), the U.S. Department of Energy (grant DE-FG02-03ER63684), and in-kind contributions from the Great Mountain Forest Corporation, Connecticut.

## References

- Aranibar, J. N., A. J. Berry, W. J. Riley, D. E. Pataki, B. E. Law, and J. R. Ehleringer (2006), Combining meteorology, eddy fluxes, isotope measurements, and modeling to understand environmental controls of carbon isotope discrimination at the canopy scale, *Global Change Biol.*, *12*, 710–730.
- Baldocchi, D. (1988), A multi-layer model for estimating sulphur dioxide deposition to a deciduous oak forest canopy, *Atmos. Environ.*, *22*, 869–884.
- Baldocchi, D. D., and D. R. Bowling (2003), Modeling the discrimination of <sup>13</sup>CO<sub>2</sub> above and within a temperate broad-leaved forest canopy on hourly to seasonal time scales, *Plant Cell Environ.*, *26*, 231–244.
- Battle, M., et al. (2000), Global carbon sinks and their variability inferred from atmospheric O<sub>2</sub> and <sup>13</sup>C, *Science*, *287*, 2467–2470.
- Bowling, D. R., P. P. Tans, and R. K. Monson (2001), Partitioning net ecosystem carbon exchange with isotopic fluxes of CO<sub>2</sub>, *Global Change Biol.*, *7*, 127–145.
- Brutsaert, W. (1975), The roughness length for water vapor, sensible heat, and other scalars, *J. Atmos. Sci.*, *32*, 2028–2031.
- Campbell, G. S. (1977), *An Introduction to Environmental Biophysics*, 159 pp., Springer, Berlin.
- Cappa, C. D., M. B. Hendricks, D. J. DePaolo, and R. C. Cohen (2003), Isotopic fractionation of water during evaporation, *J. Geophys. Res.*, *108*(D16), 4525, doi:10.1029/2003JD003597.
- Cernusak, L. A., J. S. Pate, and G. D. Farquhar (2002), Diurnal variation in the stable isotope composition of water and dry matter in fruiting *Lupinus angustifolius* under field conditions, *Plant Cell Environ.*, *25*, 893–907.
- Cernusak, L. A., G. D. Farquhar, S. C. Wong, and H. Stuard-Williams (2004), Measurement and interpretation of the oxygen isotope composition of carbon dioxide respired by leaves in the dark, *Plant Physiol.*, *136*, 3350–3363.
- Chen, B., and J. M. Chen (2007), Diurnal, seasonal and interannual variability of carbon isotope discrimination at the canopy level in response to environmental factors in a boreal forest ecosystem, *Plant Cell Environ.*, *30*, 1223–1239.
- Ciais, P., P. Tans, J. White, M. Trolier, R. Francey, J. Berry, D. Randall, P. Sellers, J. Collatz, and D. Schimel (1995), Partitioning of ocean and land uptake of CO<sub>2</sub> as inferred by <sup>δ13</sup>C measurements from the NOAA Climate Monitoring and Diagnostics Laboratory Global Air Sampling Network, *J. Geophys. Res.*, *100*, 5051–5070.
- Ciais, P., et al. (1997), A three-dimensional synthesis study of <sup>δ18</sup>O in atmospheric CO<sub>2</sub>: 1. Surface fluxes, *J. Geophys. Res.*, *102*, 5857–5872.
- Craig, H., and L. I. Gordon (1965), Deuterium and oxygen-18 variations in the ocean and the marine atmosphere, in *Stable Isotopes in Oceanographic Studies and Paleotemperatures*, edited by E. Tongiorgi, pp. 9–130, Lab. di Geol. Necl., Pisa, Italy.
- Cuntz, M., P. Ciais, G. Hoffmann, and W. Knorr (2003), A comprehensive global three-dimensional model of <sup>18</sup>O in atmospheric CO<sub>2</sub>: 1. Validation of surface processes, *J. Geophys. Res.*, *108*(D17), 4527, doi:10.1029/2002JD003153.
- Dai, A. (2007), A recent changes in factors controlling atmospheric moisture demand, *Eos Trans. AGU*, *88*(52), Fall Meet. Suppl., Abstract H34D-01.
- Denmead, O. T., and E. F. Bradley (1985), Flux-gradient relationships in a forest canopy, in *The Forest-Atmospheric Interaction*, edited by B. A. Hutchison and B. B. Hicks, pp. 421–442, D. Reidel, Dordrecht, Netherlands.
- Dongmann, G., H. W. Nünberg, H. Föstel, and K. Wagener (1974), On the enrichment of H<sub>2</sub><sup>18</sup>O in the leaves of transpiring plants, *Radiat. Environ. Biophys.*, *11*, 41–52.
- Farquhar, G. D., and J. Lloyd (1993), Carbon and oxygen isotope effects in the exchange of carbon dioxide between terrestrial plant and the atmosphere, in *Carbon and Oxygen Isotope Effects in the Exchange of Carbon Dioxide Between Terrestrial Plants and the Atmosphere*, edited by J. R. Ehleringer et al., chap. 5, pp. 47–70, Academic, San Diego, Calif.
- Farquhar, G. D., J. R. Ehleringer, and K. T. Hubick (1989), Carbon isotope discrimination and photosynthesis, *Annu. Rev. Plant Physiol. Plant Mol. Biol.*, *40*, 503–537.
- Farquhar, G. D., et al. (1993), Vegetation effects on the isotope composition of oxygen in atmospheric CO<sub>2</sub>, *Nature*, *363*, 439–443.
- Flanagan, L. B., J. P. Comstock, and J. R. Ehleringer (1991), Comparison of modeled and observed environmental influences on the stable oxygen and hydrogen isotope composition of leaf water in *Phaseolus vulgaris* L., *Plant Physiol.*, *96*, 588–596.
- Flanagan, L., B. J. R. Brooks, G. T. Varney, and J. R. Ehleringer (1997), Discrimination against C<sup>18</sup>O<sup>16</sup>O during photosynthesis and the oxygen isotope ratio of respired CO<sub>2</sub> in boreal forest ecosystems, *Global Biogeochem. Cycles*, *11*, 83–98.

- Fuentes, J. D., T. J. Gillespie, G. den Hartog, and H. H. Newmann (1992), Ozone deposition onto a deciduous forest during dry and wet conditions, *Agric. For. Meteorol.*, **62**, 1–18.
- Garratt, J. R. (1992), *The Atmospheric Boundary Layer*, 316 pp., Cambridge Univ. Press, New York.
- Gillon, J. S., and D. Yakir (2000a), Internal conductance to CO<sub>2</sub> diffusion and C<sup>18</sup>O discrimination in C<sub>3</sub> leaves, *Plant Physiol.*, **123**, 201–213.
- Gillon, J. S., and D. Yakir (2000b), Naturally low carbonic anhydrase activity in C<sub>4</sub> and C<sub>3</sub> plants limits discrimination against C<sup>18</sup>O during photosynthesis, *Plant Cell Environ.*, **23**, 903–915.
- Gillon, J., and D. Yakir (2001), Anhydrase activity in terrestrial vegetation on the <sup>18</sup>O content of atmospheric CO<sub>2</sub>, *Science*, **291**, 2584–2587.
- Grace, J., et al. (1995), Fluxes of carbon dioxide and water vapor over an undisturbed tropical forest in south-west Amazonia, *Global Change Biol.*, **1**, 1–12.
- Griffis, T. J., et al. (2005), Feasibility of quantifying ecosystem-atmosphere C<sup>18</sup>O<sup>16</sup>O exchange using laser spectroscopy and the flux-gradient method, *Agric. For. Meteorol.*, **135**, 44–60.
- Griffis, T. J., J. Zhang, J. M. Baker, N. Kljun, and K. Billmark (2007), Determining carbon isotope signatures from micrometeorological measurements: Implications for studying biosphere-atmosphere exchange processes, *Boundary Layer Meteorol.*, **123**, 295–316.
- Griffis, T. J., S. D. Sargent, J. M. Baker, X. Lee, B. D. Tanner, J. Greene, E. Swiatek, and K. Billmark (2008), Direct measurement of biosphere-atmosphere isotopic CO<sub>2</sub> exchange using the eddy covariance technique, *J. Geophys. Res.*, **113**, D08304, doi:10.1029/2007JD009297.
- Harwood, K. G., J. S. Gillon, A. Roberts, and H. Griffiths (1999), Determinants of isotopic coupling of CO<sub>2</sub> and water vapour within a *Quercus petraea* forest canopy, *Oecologia*, **119**, 109–119.
- Hoffmann, G., et al. (2004), A model of the Earth's Dole effect, *Global Biogeochem. Cycles*, **18**, GB1008, doi:10.1029/2003GB002059.
- Kaplan, J. O., I. C. Prentice, and N. Buchmann (2002), The stable carbon isotope composition of the terrestrial biosphere: Modeling at scales from the leaf to the global, *Global Biogeochem. Cycles*, **16**(4), 1060, doi:10.1029/2001GB001403.
- Kelliher, F. M., R. Leuning, M. R. Raupach, and E.-D. Schulze (1995), Maximum conductances for evaporation from global vegetation types, *Agric. For. Meteorol.*, **73**, 1–16.
- Lai, C. T., J. R. Ehleringer, B. J. Bond, and K. T. U. Paw (2005), Contributions of evaporation, isotopic non-steady state transpiration, and atmospheric mixing on the δ<sup>18</sup>O of water vapor in Pacific Northwest coniferous forests, *Plant Cell Environ.*, **29**, 77–94.
- Lamaud, E., Y. Brunet, A. Labatut, A. Lopez, J. Fontan, and A. Druihlet (1994), The Landes experiment: Biosphere-atmosphere exchanges of ozone and aerosol particles above a pine forest, *J. Geophys. Res.*, **99**, 16,511–16,521.
- Lee, X. (2000), Air motion within and above forest vegetation in non-ideal conditions, *For. Ecol. Manage.*, **135**, 3–18.
- Lee, X. (2003), Fetch and footprint of turbulent fluxes over vegetation stands with elevated sources, *Boundary Layer Meteorol.*, **107**, 561–579.
- Lee, X., S. Sargent, R. Smith, and B. Tanner (2005), In-situ measurement of the water vapor <sup>18</sup>O/<sup>16</sup>O isotope ratio for atmospheric and ecological applications, *J. Atmos. Oceanic Technol.*, **22**, 555–565.
- Lee, X., K. Kim, and R. Smith (2007), Temporal variations of the isotopic signal of the whole-canopy transpiration in a temperate forest, *Global Biogeochem. Cycles*, **21**, GB3013, doi:10.1029/2006GB002871.
- Lloyd, J., and G. D. Farquhar (1994), <sup>13</sup>C discrimination during CO<sub>2</sub> assimilation by the terrestrial biosphere, *Oecologia*, **99**, 201–215.
- Lloyd, J., et al. (1996), Vegetation effects on the isotopic composition of atmospheric CO<sub>2</sub> at local and regional scales: Theoretical aspects and a comparison between rain forest in Amazonia and a boreal forest in Siberia, *Aust. J. Plant Physiol.*, **23**, 371–399.
- Magnani, F., S. Leonardi, R. Tognetti, J. Grace, and M. Borghetti (1998), Modeling the surface conductance of a broad-leaf canopy: Effects of partial decoupling from the atmosphere, *Plant Cell Environ.*, **21**, 867–879.
- McDowell, N., et al. (2008), Measuring and modeling the stable isotope composition of biosphere-atmosphere CO<sub>2</sub> exchange: Where are we and where are we going?, *Eos Trans. AGU*, **89**(10), 94–95.
- Merlivat, L. (1978), Molecular diffusivities of H<sub>2</sub><sup>16</sup>O, HD<sup>16</sup>O, and H<sub>2</sub><sup>18</sup>O in gases, *J. Chem. Phys.*, **69**, 2864–2871.
- Merlivat, L., and J. Jouzel (1979), Global climate interpretation of the deuterium-oxygen-18 relationship for precipitation, *J. Geophys. Res.*, **20**, 5029–5033.
- Ogée, J., P. Peylin, P. Ciais, T. Bariac, Y. Brunet, P. Berbigier, C. Roche, P. Richard, G. Bardoux, and J.-M. Bonnefond (2003), Partitioning net ecosystem carbon exchange into net assimilation and respiration using <sup>13</sup>CO<sub>2</sub> measurements: A cost-effective sampling strategy, *Global Biogeochem. Cycles*, **17**(2), 1070, doi:10.1029/2002GB001995.
- Peylin, P., et al. (1996), <sup>18</sup>O in atmospheric CO<sub>2</sub> simulated by a 3D transport model: A sensitivity study to vegetation and soil fractionation factors, *Phys. Chem. Earth*, **21**, 463–469.
- Randerson, J. T., et al. (2002), Carbon isotope discrimination of Arctic and boreal biomes inferred from remote atmospheric measurements and a biosphere-atmosphere model, *Global Biogeochem. Cycles*, **16**(3), 1028, doi:10.1029/2001GB001435.
- Raupach, M. R. (1989), A practical Lagrangian method for relating scalar concentrations to source distributions in vegetation canopies, *Q. J. R. Meteorol. Soc.*, **115**, 609–632.
- Riley, W. J., C. J. Still, M. S. Torn, and J. A. Berry (2002), A mechanistic model of H<sub>2</sub><sup>18</sup>O and C<sup>18</sup>O fluxes between ecosystems and the atmosphere: Model description and sensitivity analyses, *Global Biogeochem. Cycles*, **16**(4), 1095, doi:10.1029/2002GB001878.
- Roden, J. S., and J. R. Ehleringer (1999), Observations of hydrogen and oxygen isotopes in leaf water confirm the Craig-Gordon model under wide-ranging environmental conditions, *Plant Physiol.*, **120**, 1165–1173.
- Roderick, M. L., L. D. Rotstain, G. D. Farquhar, and M. T. Hobbins (2007), On the attribution of changing pan evaporation, *Geophys. Res. Lett.*, **34**, L17403, doi:10.1029/2007GL031166.
- Santer, B. D., et al. (2007), Identification of human induced changes in atmospheric moisture content, *Proc. Natl. Acad. Sci. U. S. A.*, **104**, 15,248–15,253.
- Seibt, U., L. Wingate, and J. A. Berry (2007), Nocturnal stomatal conductance effects on the δ<sup>18</sup>O signature of foliage gas exchange observed in two forest ecosystems, *Tree Physiol.*, **27**, 585–595.
- Shuttleworth, W. J., and R. J. Gurney (1990), The theoretical relationship between foliage temperature and canopy resistance in sparse crops, *Q. J. R. Meteorol. Soc.*, **116**, 497–519.
- Suits, N. S., A. S. Denning, J. A. Berry, C. J. Still, J. Kaduk, J. B. Miller, and I. T. Baker (2005), Simulation of carbon isotope discrimination of the terrestrial biosphere, *Global Biogeochem. Cycles*, **19**, GB1017, doi:10.1029/2003GB002141.
- Tans, P. P. (1980), On calculating the transfer of <sup>13</sup>C in reservoir models of the carbon-cycle, *Tellus*, **32**, 464–469.
- Tans, P. P. (1998), Oxygen isotopic equilibrium between carbon dioxide and water in soils, *Tellus, Ser. B*, **58**, 163–178.
- Welp, L. R., X. Lee, K. Kim, T. J. Griffis, K. Billmark, and J. M. Baker (2008), δ<sup>18</sup>O of water vapor, evapotranspiration and the sites of leaf water evaporation in a soybean canopy, *Plant Cell Environ.*, **31**, 1214–1228.
- Wesely, M. L., and B. B. Hicks (1877), Some factors that affect the deposition rates of sulfur dioxide and similar gases in vegetation, *J. Air Pollut. Control Assoc.*, **21**, 1110–1116.
- Willett, K. M., N. P. Gillett, P. D. Jones, and P. W. Thorne (2007), Attribution of observed surface humidity changes to human influence, *Nature*, **449**, 710–713.
- Williams, D. G., et al. (2004), Evapotranspiration components determined by stable isotope, sap flow and eddy covariance techniques, *Agric. For. Meteorol.*, **125**, 241–258.

J. M. Baker, K. A. Billmark, and T. J. Griffis, Department of Soil, Water, and Climate, University of Minnesota, St. Paul, MN 55108, USA.

K. Kim, X. Lee, and L. R. Welp, School of Forestry and Environmental Studies, Yale University, 21 Sachem Street, New Haven, CT 06510, USA. (xuhui.lee@yale.edu)